



**People`s Democratic Republic of Algeria**

**Ministry of Higher Education and Scientific Research**

**University of Echahid Hamma Lakhdar - El Oued**

**Faculty of Technology**

**Department of Mechanical Engineering**

**Dissertation**

**ACADEMIC MASTER**

**Domain:** Science and Technology

Division: Electromechanics

Specialty: Electromechanics

**Presented by:**

- 1. OUSSAMA LOUHIDI**
- 2. ALLAG BRAHIM**

**Entitled:**

**A Hybrid Approach to PMSMs and Wind Turbine  
Optimization: Combining (FOC) with Model Predictive Control**

Dissertation Submitted in Partial Fulfillment of the Requirements for the Master *Electromechanics*

Publicly defended in: ...../...../2025

Board of Examiners:

**Dr. CHABANI MOHAMED ALSASI**

**Chairman**

**Dr. HAMZA MESAI AHMED**

**Examiner**

**Dr. BENAMOR Afaf**

**Supervisor**

**Academic Year: 2024/2025**



## Abstract

This work presents a study of the control of the permanent magnet synchronous machine (PMSMs) in the context of energy conversion associated with the techniques of Field Oriented Control (FOC) and model predictive control (MPC). In the firstly part of our thesis, modeling a wind power conversion chain using a Permanent Magnet Synchronous Machine (PMSM) is presented. The use of the permanent magnet synchronous wind generator makes variable speed wind energy conversion systems more attractive than fixed speed ones because of the possibility of optimal energy extraction under different operating conditions, with the use of the voltage MLI rectifier modeling. The secondly part of this work, is concerned with the application of Field Oriented Control (FOC) and predictive control (MPC) in our energy conversion system as the control strategy applied. On the other hand, the switching frequency is uncontrollable as MLI rectifier at the voltage level  $V_{dc}$  are important. In order to improve this structure and provide good dynamics of the  $V_{dc}$  voltage, we have associated (PMSGs) predictive control (MPC), where the system is subjected to parameter variations. To validate the performance of this type of control, simulation tests are carried out. The simulation results found are analyzed to show the performance of this type of control.

**Keywords:** Wind power, Permanent Magnet Synchronous PMSM, Wind turbine, Rectifier with MLI, Field Oriented Control (FOC), model predictive control (MPC).

## الملخص:

يعرض هذا العمل دراسة حول التحكم في الآلة التزامنية ذات المغناطيس الدائم (PMSM) المستخدمة في أنظمة الرياح، وذلك في سياق تحويل الطاقة بالاعتماد على تقنيتي التحكم المتجه الموجه (FOC) والتحكم التنبؤي (MPC). في الجزء الأول من هذا العمل، تم تقديم نمذجة لسلسلة تحويل طاقة الرياح باستخدام آلة تزامنية ذات مغناطيس دائم (PMSM). إن استخدام هذا النوع من المولدات يجعل أنظمة تحويل طاقة الرياح ذات السرعة المتغيرة أكثر جاذبية من نظيرتها ذات السرعة الثابتة، نظرًا لإمكانية استخراج الطاقة بشكل أمثل تحت ظروف تشغيل مختلفة، مع الأخذ بعين الاعتبار نمذجة المقوم من نوع MLI على مستوى الجهد. أما الجزء الثاني من العمل، فيتعلق بتطبيق تقنيتي التحكم المتجه الموجه (FOC) والتحكم التنبؤي (MPC) ضمن منظومة تحويل الطاقة المقترحة، باعتبارهما استراتيجيات للتحكم من جهة أخرى، فإن تردد التبديل غير قابل للتحكم في حالة استخدام المقوم MLI على مستوى جهد  $V_{dc}$ ، مما يجعل من الضروري تحسين هذه البنية لتحقيق ديناميكية جيدة للجهد  $V_{dc}$  ولهذا الغرض، تم ربط تقنية التحكم التنبؤي (MPC) بالآلة التزامنية ذات المغناطيس الدائم (PMSM) لمواجهة تغيرات المعاملات. للتحقق من فعالية هذا النوع من التحكم، تم إجراء اختبارات محاكاة وتحليل النتائج بهدف تقييم أداء المنظومة.

**الكلمات المفتاحية:** طاقة الرياح، الآلة التزامنية ذات المغناطيس الدائم PMSM، التوربينات الريحية، مقوم MLI، التحكم المتجه الموجه (FOC)، التحكم التنبؤي (MPC).

# *Acknowledgment*

*We give thanks to God for having given us the courage and the conscience to carry out this work. First of all, our deep gratitude to our supervisor **Dr. BENAMOR Afaf**, Professor at Hama Lakhdar University of El-Oued, for having supervised our thesis and her availability. Our valiant thanks to all those who have contribute from near or far, directly or indirectly, particularly our colleagues and our family for having trust as well as their valuable advice and encouragement throughout the years, in a continuous or occasional manner, to the successful completion of this work.*

*Thank you to all of you.*

*From the number of students:*

*ALLAG Brahim*

*LOUHIDI Oussama*

# Table of contents

<b>TABLE OF CONTENTS .....</b>	<b>II</b>
<b>LISTS OF FIGURES .....</b>	<b>IV</b>
<b>GENERAL INTRODUCTION.....</b>	<b>1</b>
<b>I CHAPTER I: GENERALITIES OF THE (PMSM) MACHINE AND WIND TURBINE.....</b>	<b>4</b>
I.1 INTRODUCTION.....	4
I.2. BRIEF HISTORY OF WIND TURBINE.....	4
I.3. GENERALITY OF WIND TURBINE.....	5
I.3.1. Wind turbine.....	5
I.3.2. Operating principle of wind turbines.....	6
I.3.3. Wind turbine components.....	6
I.4. WIND RESOURCES.....	7
I.4.1. NATURE OF THE WIND.....	7
I.4.2. Geographical variation in the wind resource.....	7
I.4.3. Long-term wind speed variations.....	8
I.4.4. Gust wind speeds.....	8
I.4.5. Wind speed prediction and forecasting.....	8
I.5. TYPES AND CLASSIFICATIONS OF WIND TURBINES.....	9
I.5.1. Vertical axis wind turbines.....	9
I.5.2. Horizontal axis wind turbines.....	9
I.6. TYPES OF WIND ENERGY CONVERSION SYSTEMS.....	10
I.6.1. Fixed speed wind turbines.....	10
I.6.2. Variable speed wind turbines.....	11
I.7. APPLICATION OF WIND TURBINE CONVERTERS.....	11
I.8. CONFIGURATIONS OF VARIABLE SPEED WECS.....	11
I.8.1. Synchronous Generator.....	12
I.8.2. Asynchronous generator.....	13
I.8.3. Asynchronous squirrel cage machine.....	13
I.8.4. Double-fed asynchronous machine of the "wound rotor".....	14
I.8.5. Permanent Magnetic Synchronous Generator System.....	15
I.9. ADVANTAGES AND DISADVANTAGES OF WIND TURBINES.....	15
I.9.1. Advantages of Wind Turbine.....	15
I.9.2. Disadvantages of Wind Turbine.....	16
I.10. THE PERMANENT MAGNET SYNCHRONOUS MACHINES (PMSMS).....	16
I.10.1. Operating principle (PMSM).....	17
I.10.2. Torque of permanent magnet synchronous machines.....	18
I.11. ADVANTAGES OF PERMANENT MAGNET SYNCHRONOUS MACHINES (PMSM).....	18
I.12. DISADVANTAGES OF PERMANENT MAGNET SYNCHRONOUS MACHINES (PMSM).....	19
I.13. APPLICATIONS OF (PMSM) IN RENEWABLE ENERGY SYSTEMS.....	19
I.15. CONCLUSION.....	21
<b>II CHAPTER II: MODELING OF WIND ENERGY SYSTEM COMPONENTS .....</b>	<b>22</b>
II.1. INTRODUCTION.....	23
II.2. MODELING OF THE PERMANENT MAGNET SYNCHRONOUS MACHINE.....	23
II.1.1 Equation of the PMSM model.....	23
II.1.2 Machine equation in the Park frame ( $d, q$ ).....	25

II.1.3	<i>Transition from the <math>d q</math> frame to the <math>\alpha \beta</math> frame</i>	26
II.1.4	<i>Application of the Park transformation to PMSM</i>	27
II.2	EXPRESSION OF THE ELECTROMAGNETIC TORQUE	27
II.3	FORMATION OF STATE EQUATION	28
II.4	MODELING OF PMSM BY MATLAB/SIMULINK	28
II.5	MODELING OF THE WIND TURBINE	29
II.5.1	<i>Wind Modeling</i>	30
II.5.2	<i>Modeling of a Horizontal-Axis Wind Turbine</i>	30
II.5.2.1	Modeling of the turbine	31
II.5.2.2	Multiplier Model	33
II.5.2.3	Dynamic Equation of the blade (arbre)	33
II.6	WIND TURBINE MODEL IN MATLAB/SIMULINK	34
II.7	MODELING OF A PWM VOLTAGE RECTIFIER	35
II.7.1	<i>Operating principle of a PWM rectifier MLI</i>	36
II.8	CONCLUSION:	37
<b>III</b>	<b>CHAPTER III: CONTROL OF PMSM AND THE PROPOSED HYBRID STRATEGY</b>	<b>39</b>
III.1	INTRODUCTION	40
III.2	FIELD-ORIENTED CONTROL	40
III.3	ADVANTAGES AND DISADVANTAGES OF FIELD-ORIENTED CONTROL	40
III.3.1	<i>Advantages of Field-Oriented Control</i>	40
III.3.2	<i>Disadvantages of Field-Oriented Control</i>	41
III.4	THE PRINCIPLE OF FIELD-ORIENTED CONTROL FOR PMSM	41
III.5	STRATEGY OF VECTOR CONTROL FOR PMSM	42
III.6	DECOUPLING BY COMPENSATION	43
III.7	FIELD-ORIENTED CONTROL OF PMSM	46
III.7.1	<i>Global Diagram of the Field-Oriented Control for the (PMSM)</i>	46
III.7.2	<i>Regulator design</i>	47
III.7.2.1	Regulator Tuning	48
III.8	HISTORY OF PREDICTIVE CONTROL	51
III.9	PRINCIPLE OF PREDICTIVE CONTROL	51
III.10	ADVANTAGES OF MODEL PREDICTIVE CONTROL (MPC)	53
III.11	MODEL FORMULATION	53
III.12	PREDICTOR DEVELOPMENT	55
III.13	OPTIMIZATION CRITERION	56
III.14	DESIGN OF MODEL PREDICTIVE CONTROL FOR PMSM	57
III.15	STRUCTURE OF THE PREDICTIVE CONTROL ALGORITHM FOR THE INVERTER	58
III.16	MODEL FOC AND MPC OF THE PMSGs BY MATLAB/SIMULINK	59
III.17	SIMULATION RESULTS	59
III.18	CONCLUSION	63
	<b>CONCLUSION</b>	<b>64</b>
	<b>REFERENCES</b>	<b>66</b>
	<b>ANNEXE</b>	<b>71</b>

# *Lists of figures*

FIGURE.I.1. ENERGY RESOURCES. ....	5
FIGURE.I.2. RENEWABLE ENERGY SOURCE. ....	5
FIGURE.I.3. WIND TURBINE COMPONENTS. ....	6
FIGURE.I.4. DIFFERENT TYPES OF VERTICAL AXIS WIND TURBINES. ....	9
FIGURE.I.5. CHARACTERISTIC CURVES OF AVERAGED POWER COEFFICIENT AS A FUNCTION OF TIP SPEED RATIO FOR VARIOUS WIND TURBINES. ....	10
FIGURE.I.6. CONSTANT SPEED WIND ENERGY CONVERSION SYSTEM. ....	11
FIGURE.I.7. VARIABLE SPEED WIND TURBINE BASED ON THE CAGE ASYNCHRONOUS MACHINE. ....	11
FIGURE.I.8. VARIABLE SPEED WIND TURBINE BASED ON THE CAGE ASYNCHRONOUS MACHINE. ....	13
FIGURE.I.9. VARIABLE SPEED WIND TURBINE BASED ON THE CAGE ASYNCHRONOUS MACHINE. ....	13
FIGURE.I.10. MULTIPLE-STAGE GEARED SCIG CONCEPT WITH FULL-SCALE CONVERTER. ....	14
FIGURE.I.11. VARIABLE SPEED CONCEPT WITH DFIG. ....	14
FIGURE I.12. DIFFERENT TYPES OF ROTOR OF AN (PMSMS). ....	17
FIGURE I.13. OPERATING PRINCIPLE OF THE PERMANENT MAGNET MOTOR. ....	17
FIGURE II.1. REPRESENTATION OF A PERMANENT MAGNET SYNCHRONOUS MACHINE. ....	24
FIGURE.II.2. EQUIVALENT REPRESENTATION IN THE PARK FRAME. ....	26
FIGURE.II.3. MODELING OF PMSM BY MATLAB/SIMULINK. ....	29
FIGURE.II.4. SCHEMA DE LA TURBINE EOLIENNE. ....	29
FIGURE.II.5. SIMPLIFIED MECHANICAL MODEL OF THE TURBINE. ....	31
FIGURE.II.6. POWER COEFFICIENT $C_p$ AS A FUNCTION OF THE TIP SPEED RATIO $\lambda$ . ....	32
FIGURE.II.7. BLOCK DIAGRAM OF THE WIND TURBINE MODEL. ....	34
FIGURE.II.8. BLOCK MODEL OF THE WIND TURBINE. ....	34
FIGURE.II.9. BASIC TOPOLOGIES OF A VOLTAGE RECTIFIER. ....	36
FIGURE.II.10. PWM RECTIFIER BLOCK DIAGRAM BY MATLAB/SIMULINK. ....	37
FIGURE.II.11. PWM RECTIFIER VOLTAGE $V_{dc}$ . ....	37
FIGURE III.1. THE PRINCIPLE OF FIELD-ORIENTED CONTROL. ....	42
FIGURE III.2. GENERAL STRUCTURE: (MACHINE-DECOUPLING BY COMPENSATION). ....	43
FIGURE III.3. DESCRIPTION OF THE COUPLINGS. ....	45
FIGURE III.4. PRINCIPLE OF DECOUPLING BY COMPENSATION. ....	45
FIGURE III.5. GLOBAL DIAGRAM OF THE FIELD-ORIENTED CONTROL FOR THE (PMSM). ....	46

FIGURE III.6 .PI REGULATOR DESIGN .....	48
FIGURE III.7. $I_q$ CURRENT CONTROL LOOP .....	49
FIGURE III.8. CURRENT REGULATION LOOP OF $I_D$ .....	50
FIGURE III.9. PRINCIPLE OF PREDICTIVE CONTROL .....	52
FIGURE III.10. DIGITAL REPRESENTATION MODEL FOR THE GPC. ....	54
FIGURE III.11. PRINCIPLE DIAGRAM OF PREDICTIVE CONTROL.....	58
FIGURE III.12. MODEL FOC OF THE PMSGs BY MATLAB/SIMULINK.....	59
FIGURE III.13. MODEL MPC OF THE PMSGs BY MATLAB/SIMULINK.....	59
FIGURE. III.14. VOLTAGES $V_{abc}$ IN TWO SIMULATION CASES.....	59
FIGURE. III.15. VOLTAGES $V_{abc}$ IN TWO SIMULATION CASES WITH ZOOM. ....	61
FIGURE. III.16. CURRENT $I_{abc}$ IN TWO SIMULATION CASES. ....	61
FIGURE. III.17. CURRENT $I_{abc}$ IN TWO SIMULATION CASES WITH ZOOM.....	61
FIGURE. III.18. VOLTAGE $V_{dq}$ $I_{abc}$ IN TWO SIMULATION CASES. ....	62
FIGURE. III.19. CURRENT $I_{dq}$ IN TWO SIMULATION CASES.....	62
FIGURE. III.20. VOLTAGE $V_{dc}$ IN TWO SIMULATION CASES. ....	63
FIGURE. III.21. MECHANICAL SPEED. ....	63

## *General Introduction*

The world's energy needs are increasing at an accelerating pace across all regions. The excessive dependence on energy imports from a small number of countries—most of which are politically unstable—along with the volatility of oil and gas prices, results in a precarious energy supply situation that already poses a heavy burden on the global economy.

Furthermore, the harmful effects of fossil fuels on the environment add another dimension to this problem. Power plants release gases into the atmosphere that cause the greenhouse effect, along with particles that create urban heat islands—one of the main causes of climate change.

The increasing demand for clean, reliable, and sustainable energy has driven significant advancements in renewable energy technologies. Among these, wind energy has emerged as one of the most promising and rapidly expanding sources. Efficient utilization of wind energy requires advanced control strategies to ensure the reliable and optimal operation of wind turbine systems, particularly those incorporating Permanent Magnet Synchronous Machines (PMSMs), known for their high efficiency, power density, and dynamic performance.

The Permanent Magnet Synchronous Motor (PMSM) is a type of electric motor that uses permanent magnets in the rotor instead of excitation windings. This motor is characterized by high efficiency and high power density, along with precise control of speed and torque, making it suitable for various applications such as electric vehicles, robotics, and renewable energy systems. Due to its design, the PMSM offers excellent dynamic performance and fast response.

Controlling PMSM applications poses several challenges, including nonlinear system dynamics, varying operating conditions, and the need for real-time adaptability. Traditionally, Field-Oriented Control (FOC) has been widely adopted due to its ability to decouple torque and flux control, mimicking the behavior of DC machines and providing robust dynamic performance.

The Model Predictive Control (MPC) an advanced control strategy that predicts future behavior based on a dynamic model of the system and optimizes control inputs accordingly. MPC offers superior handling of constraints, system nonlinearities, and multi-variable interactions, making it a powerful candidate for renewable energy systems.

The main objective of this work, are Field-Oriented Control (FOC) and Model Predictive Control (MPC) represents, especially in systems demanding high precision and efficient response. FOC works by decomposing the current into magnetic and torque components, enabling precise control over the motor's torque and speed, similar to DC motor control, thus providing smooth operation and good dynamic response. Introduced in the late 80s, MPC is considered one of the most popular predictive control methods, particularly in industrial processes. MPC is based on the minimization of a quadratic cost function over a receding horizon and depends on four key parameters: the minimum and maximum prediction horizons, the control horizon, and the control weighting factor. Integrating these two methods into a hybrid control system allows benefiting from the instantaneous accuracy of FOC combined with the flexibility of MPC to optimize performance under system constraints and manage uncertainties and disturbances, thereby enhancing system stability and operational efficiency.

The objective also of this work, presented within the framework of this MASTERACADEMY thesis, A Hybrid Approach to PMSMs and Wind Turbine Optimization: Combining (FOC) with Model Predictive Control (MPC).

Starting from the regulation of the DC bus voltage introduced by the AC/DC converter, and passing through the control of the permanent magnet synchronous generator, all the results were obtained through simulation using MATLAB/Simulink software.

To do this, the writing of the thesis is organized as follows:

In a first chapter, presents an overview of wind turbines and Permanent Magnet Synchronous Machines (PMSMs) within renewable energy systems. It begins with the historical development of wind energy and the principles behind wind turbine operation. Different types of turbines, including vertical and horizontal axis designs, are compared. The chapter explains how wind variability affects energy production and the importance of accurate forecasting.

Chapter Two represents a fundamental step toward developing an effective control system for the Permanent Magnet Synchronous Machine (PMSM). This chapter focuses on constructing an accurate mathematical model of the machine. Next, the modeling of the wind turbine and the PWM-based AC/DC converter will be presented in the second part of the chapter. Finally, the simulation results will be discussed.

Chapter Three presents two advanced control strategies for Permanent Magnet Synchronous Machines (PMSMs): Field-Oriented Control (FOC) and Model Predictive Control (MPC). FOC

decouples torque and flux control, enabling dynamic performance similar to DC machines, while MPC predicts system behavior in real time to optimize control actions under constraints. The chapter details the principles, advantages, and implementation of both methods, then applies them to PMSM systems using a voltage-source inverter. This analysis provides a foundation for combining FOC and MPC into hybrid control approaches to improve efficiency and robustness.

Finally, we conclude this work with a general conclusion, followed by some perspectives for the continuation of this research in the future.

# **Chapter I: Generalities of the (PMSM) Machine and Wind Turbine**

## **I.1 Introduction**

Wind energy is a major source of renewable energy, generated by differences in atmospheric pressure and classified into global winds, which cover large-scale movements, and local winds, which are confined to specific regions. Wind turbines are widely used to convert wind kinetic energy into electricity, despite the challenges posed by high initial investment costs, which have significantly decreased in recent years. In this context, Permanent Magnet Synchronous Machines (PMSMs) are gaining increasing attention due to their role in renewable energy systems, such as wind and wave energy, in addition to their growing adoption in electric transportation systems.

This special issue of *Energies* focuses on the design, modeling, and operation of PMSMs, a multidisciplinary field that encompasses electromagnetic, mechanical, and thermal management aspects. A key research trend in this area involves reducing dependence on rare earth elements by developing sustainable magnetic materials. The issue also highlights the importance of experimental validation, despite the challenges associated with prototype manufacturing and measurement processes.

## **I.2. Brief history of wind turbine**

The utilization of wind energy as a power source dates back to 5000 B.C. in ancient Egypt, where wind-driven sailboats were used for navigation along the Nile River. By the 11th century, windmills had been developed in China and the Middle East for food processing before being introduced to Europe for mechanical applications. During the Industrial Revolution, windmills remained in use, and by the late 19th century, the first attempts to generate electricity from wind energy emerged in the United States and Denmark. However, interest in wind power declined until the oil crisis of the 1970s, which prompted a renewed global focus on alternative energy sources [Abd 18].

Today, wind energy plays a crucial role in electricity generation, with significant technological advancements enhancing turbine efficiency and cost-effectiveness. By 2006, modern wind turbines were capable of producing 180 times more electricity than those installed two decades earlier at the same location, while achieving a 50% reduction in cost per kilowatt-hour [Mel 22].

### I.3. Generality of wind turbine

Renewable energy sources, such as solar, wind, and hydropower, rely on weather conditions, making their availability variable and sometimes unpredictable, which can lead to power generation disruptions in cases of supply shortages. Additionally, producing large-scale energy from renewable sources presents greater challenges compared to fossil fuel power plants, requiring the development of additional infrastructure to meet the increasing energy demand. While fossil fuels offer higher energy density and are easier to store and transport, their environmental and economic impacts have driven the transition toward sustainable energy solutions, leading to growing interest in renewable energy technologies such as solar, wind, hydropower, and biofuels. In this context, Algeria has recently begun utilizing wind energy for electricity generation by establishing its first wind farm in Kabertin, Adrar Province, consisting of twelve wind turbines with a total capacity of 10.2 MW. The site was selected based on the availability of strong winds and vast open spaces; however, sandy winds in desert regions may impact the aerodynamic performance of wind turbines, a subject that still requires further research. The Figures I.1 and I.2; have shown the renewable energy sources [Mar 16], [Sha 16], [Mel 22].

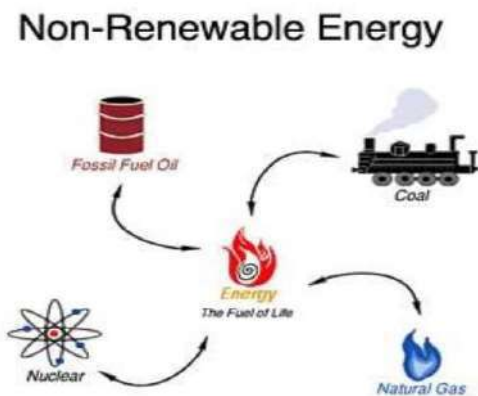


Figure.I.1. Energy resources.

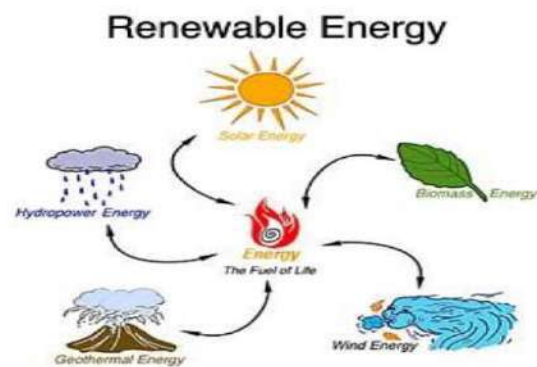


Figure.I.2. Renewable energy source.

#### I.3.1. Wind turbine

Wind turbines are devices that convert the kinetic energy of the wind into mechanical energy, which is then transformed into electrical energy through a generator. These turbines are used to produce clean and renewable energy.

### I.3.2. Operating principle of wind turbines

Wind turbines operate by capturing wind energy, converting it into mechanical power, and then generating electricity. As the wind pushes the blades, they begin to rotate, transforming the

wind's kinetic energy into rotational energy within the shaft. This rotation is then transferred to the gearbox (if present) to increase speed, and the mechanical energy is subsequently converted into electrical energy through the generator. To ensure maximum efficiency, the turbine regulates the speed and angle of the blades while adjusting the electrical voltage and frequency to match the power grid. Finally, the generated electricity is either transmitted to the power grid or used locally, passing through transformers to modify the voltage as needed [Tho 05].

### I.3.3. Wind turbine components

A modern wind turbine consists of several key components that contribute to converting wind energy into electrical energy. These components include [Jha 11], [Mel 22]:

- **Blades:** Capture wind energy and convert it into rotational motion.
- **Rotor:** Connects the blades to the main shaft and transfers the motion.
- **Gearbox:** Increases the rotational speed before transferring it to the generator (some designs eliminate this component).
- **Generator:** Converts mechanical energy into electrical energy.
- **Control System:** Regulates the turbine's operation to ensure safe and efficient performance.
- **Tower:** Elevates the turbine to an optimal height where wind speeds are higher.
- **Grid Connection System:** Converts the generated electricity to be compatible with the electrical grid.

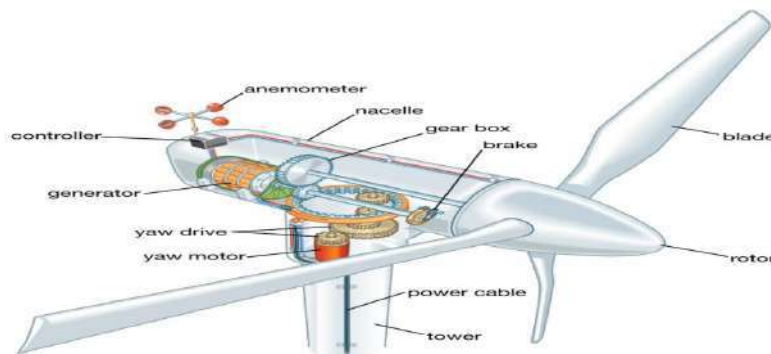


*Figure.I.3. Wind turbine components.*

## **I.4. Wind resources**

### **I.4.1. Nature of the wind**

The energy available in the wind varies proportionally to the cube of wind speed, making it essential to understand wind resource characteristics for all aspects of wind energy utilization. This includes identifying suitable locations, assessing the economic feasibility of wind farm projects, designing wind turbines, and analyzing their impact on electricity distribution networks and consumers.

Wind speed varies from one location to another depending on surface topography and altitude. Large-scale temporal variations mean that wind availability may fluctuate from year to year and even over decades, with long-term changes that are not yet fully understood. These uncertainties can make it challenging to accurately predict the economic viability of wind farm projects. On shorter timescales, seasonal variations are more predictable, although significant fluctuations still occur over even shorter periods, such as daily and hourly changes. While these short-term variations are relatively well understood, they pose challenges in wind energy forecasting and grid integration, requiring advanced control and storage solutions to balance supply and demand.

Additionally, local geographical factors, such as mountains, valleys, and water bodies, significantly influence wind patterns, making site selection a crucial factor in optimizing wind energy production. Therefore, understanding these variations is essential for improving wind turbine design, enhancing grid stability, and ensuring the long-term economic feasibility of wind energy projects [Garr 01].

### **I.4.2. Geographical variation in the wind resource**

Fundamental climatic patterns lead to clear differences between regions, and these variations are influenced by local topographical and thermal factors. Mountains and hills contribute to increased wind speeds in certain areas due to the acceleration of airflow as it moves over or around them, as well as its passage through valleys and mountain passes aligned with the wind direction. Conversely, terrain can also lead to reduced wind speeds in some locations, such as sheltered valleys or areas situated behind mountain ridges, where airflow patterns create stagnation zones. Additionally, thermal effects play a significant role in causing local climatic variations [Garr 01].

Coastal regions generally experience strong winds due to temperature differences between land and sea. When the sea is warmer than the land, a circular airflow pattern develops, with cool air moving from the land toward the sea while warm air rises over the water. When the land becomes warmer than the sea, this pattern reverses. Since land heats up and cools down more quickly than the sea, the shift between land and sea breezes occurs in a regular cycle throughout the day [Garr 01], [Abd 18].

### **I.4.3. Long-term wind speed variations**

There is evidence suggesting that wind speed at a specific location may undergo very slow long-term changes. Although accurate historical records are limited, detailed analysis—such as studies conducted in 1991—has revealed clear trends. These changes are likely associated with long-term temperature fluctuations, for which there is strong historical evidence [Garr 01].

Furthermore, ongoing discussions focus on the potential impacts of human-induced global warming on climate patterns, which will undoubtedly affect wind conditions in the coming decades. In addition to these long-term trends, wind speed at a given location may experience significant variations from year to year due to various factors. These include global climate phenomena such as El Niño, changes in atmospheric particulates caused by volcanic eruptions, sunspot activity, and more. Such fluctuations contribute to the uncertainty in accurately predicting the energy output of a wind farm over its expected operational lifespan [Abd 18].

### **I.4.4. Gust wind speeds**

Knowing the maximum gust speed that may occur within a specific time interval is useful in many situations. This is typically represented by the gust factor ( $G$ ), which is the ratio of the gust wind speed to the hourly mean wind speed. This factor is clearly influenced by turbulence intensity and is also affected by the duration of the gust. Therefore, the gust factor for a one-second gust will be higher than that of a three-second gust, as any three-second gust contains within it a shorter but more intense one-second gust [Garr 01], [Mel 22].

### **I.4.5. Wind speed prediction and forecasting**

Due to the variable nature of wind resources, the ability to predict wind speed in advance is highly important. Wind forecasts are generally divided into two main categories: short-term forecasts, which estimate turbulent fluctuations over periods ranging from seconds to minutes and help optimize the operational control of wind turbines or wind farms, and long-term

forecasts, which cover several hours or days and are used for planning the integration of other power plants into the electrical grid [Garr 01], [Abd 18].

Short-term forecasts primarily rely on statistical techniques that analyze recent data and extrapolate wind variations, while long-term forecasts benefit from meteorological models to study climate trends. Combining statistical and meteorological approaches can provide accurate and reliable predictions of wind farm performance [Mel 22].

## I.5. Types and classifications of wind turbines

Wind turbine systems are classified into two main types based on the orientation of their rotational axis and blade design: vertical-axis wind turbines (VAWT) and horizontal-axis wind turbines (HAWT) [Bri 13], [Mel 22].

### I.5.1. Vertical axis wind turbines

Vertical-axis windmills and turbines appear to be older than horizontal-axis windmills. VAWTs are categorized into drag-driven Savonius rotors and lift-driven Darrieus turbines. The straight-bladed Hrotor is a form of Darrieus turbine (Figure I.4). VAWTs have the advantage of being independent of wind direction changes. Heavy components can be installed near the ground [Mel 22],[Abd 18].

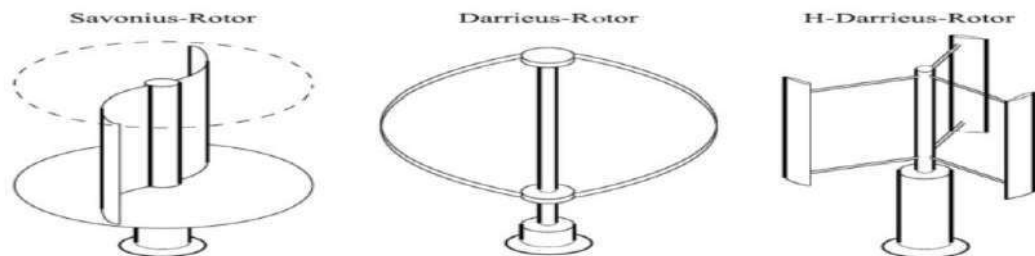


Figure.I.4. Different types of vertical axis wind turbines.

### I.5.2. Horizontal axis wind turbines

Since the entire area swept by HAWT blades always confronts the wind during operation, more wind energy can often be gathered by these blades than by VAWT blades.

HAWTs are categorized as micro-scale ( $\mu$ SWT, diameter  $f$  0.1 m), small-scale (SSWT, 0.1 m  $<$  diameter  $f$  1 m), mid-scale (MSWT, 1 m  $<$  diameter  $f$  5 m), and large-scale (LSWT, diameter  $>$  5 m) based on the blade's diameter [Bel 14],[Bri 13].

Offshore locations or wind farms are used to install large HAWTs. In residential locations, small-scale HAWTs are frequently observed. Figure.I.5. illustrates the power performance and

operating range of several wind turbine designs to provide a better understanding of various wind turbine concepts [Mel 22].

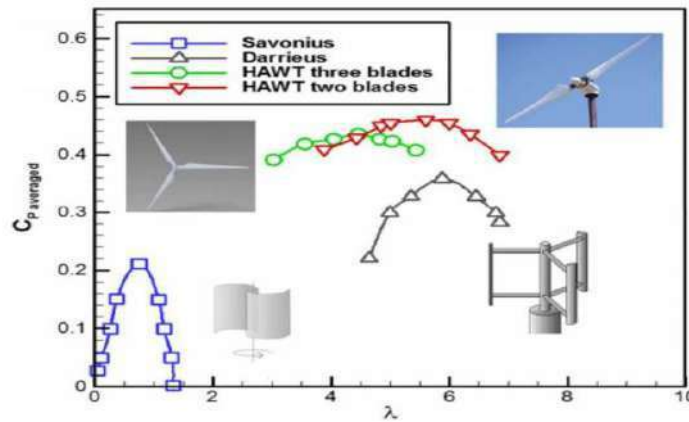


Figure.1.5. Characteristic curves of averaged power coefficient as a function of tip speed ratio for various wind turbines.

## I.6. Types of Wind Energy Conversion Systems

There are essentially two types of wind turbines. WECS, variable speed wind turbines, and fixed speed wind turbines, which primarily have a squirrel cage asynchronous generator with a rotor speed fixed to a specific speed. By adding flexibility to the system's response to abrupt changes in wind speed, this also raises the quality of the electrical power generated.

### I.6.1. Fixed speed wind turbines

In this instance, the wind turbines' rotational speed is controlled by the pitch control, or blade alignment. The primary component of these wind turbines is an asynchronous squirrel-cage machine that is directly connected to a strong energy network and forces its frequency (50 Hz) on the stator quantity. The MAS's rotation speed must be greater than synchronism (negative slip) in order to guarantee generator operation. Fixed speed systems are unable to achieve the different rotor speeds that yield the greatest value under variable wind conditions because they do not permit appreciable fluctuations in rotor speed [Abd 18], [Mel 22], [Gam 21].

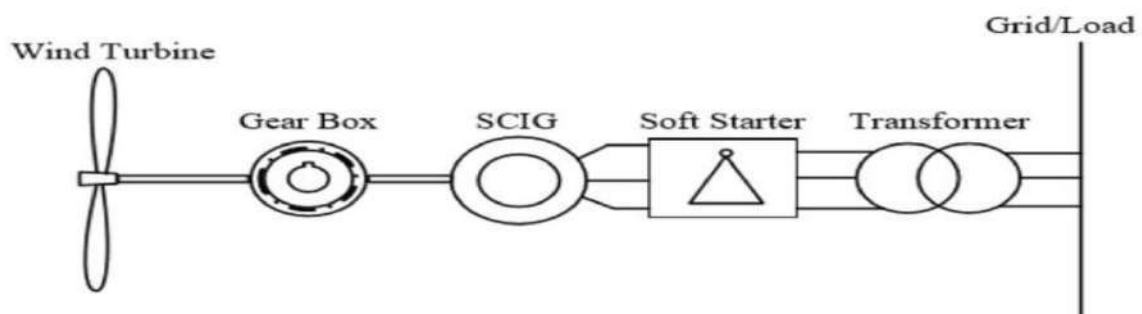


Figure.I.6. Constant Speed Wind Energy Conversion System.

## I.6.2. Variable speed wind turbines

Figure.I.7. shows the second case. Despite its simplicity, the fixed speed operating system can be noisy, due to the modification of the aerodynamic characteristics due to the orientation of the blades, and limits the range of exploitable wind speeds. A power interface adapts the frequency of the generator currents to that of the network and thus makes it possible to operate at variable speed this then makes it possible to maximize the power extracted from the wind. But in this case, a direct connection to the network is no longer possible because of the variable nature of the frequency of the stator voltages. A power electronics interface between the generator and the network is then necessary. The latter is conventionally made up of two [Mel 22], [Gam 21].

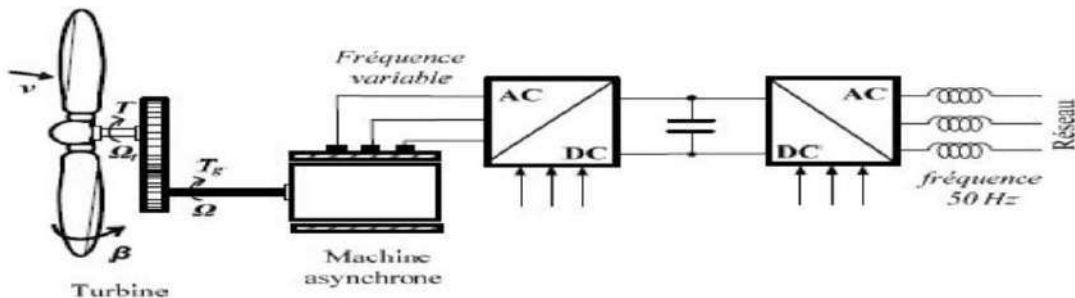


Figure.I.7. Variable speed wind turbine based on the cage asynchronous machine.

## I.7. Application of wind turbine converters

Reverse osmosis (RO), mechanical vapor compression (MVC), and electro-dialysis (ED) are three processes that can be coupled to wind turbines. Spring Field also described the use of rotational energy generated by the rotation of blades to power a mechanical device like a water pump or to generate electricity through a generator [Mel 22].

After comparing the two traditional pumping techniques, Siding found that, at average wind speeds greater than 3 m/s, the wind turbine is the most practical pumping prime mover. A wind-energy-capturing device for moving automobiles was created by Thomas et al. An electric or hybrid vehicle's motor may be powered by electrical energy that has been stored in a battery system [Tho 05].

## I.8. Configurations of variable speed WECS

Generator type is used to classify wind turbines. To ensure effective generator performance, electronic transducers must be used.

The four types of wind turbine generators are as follows:

**Type 1:** squirrel cage induction machine (almost constant speed).

**Type 2:** variable resistance rotary wound induction machine (wider speed/torque range).

**Type 3:** Rotary wound induction machine with power electronics (double feed, widest range).

**Type 4:** complete transformer interface machine (usually PMSG or other synchronous combination).

The term "machine" refers to a system that can operate either as a motor or a generator, depending on whether mechanical energy is applied to or extracted from the shaft. The gear ratio is designed to achieve the required torque-speed characteristics, while control interfaces utilize transducers programmed to follow specific torque-speed curves.

The Wind Turbine Simulator (WTS) generator presented in this study is an outdoor field synchronous machine, primarily functioning as an automotive alternator. It is classified as a type 4 configuration, incorporating a transducer interface with a basic rectifier circuit. Additionally, a boost converter can be integrated to regulate the generator's torque. This machine is widely used in wind energy applications due to its robustness and ease of implementation. However, its performance is significantly influenced by the control strategy employed. In its standard configuration, the WTS generator operates in an uncontrolled mode, where the stator terminals are rectified to produce a DC voltage and current. The output voltage [Mel 22],[Sid 97].

### **I.8.1. Synchronous Generator**

This type of machine is widely used in conventional electricity generation, especially in high-power plants such as thermal, hydraulic, and nuclear power stations. In the wind energy sector, synchronous generators with capacities ranging from 500 kW to 2 MW are significantly more expensive than induction generators of the same size.

When a synchronous generator is directly connected to the electrical grid, its speed remains fixed and follows the grid frequency. Due to this rigid connection between the generator and the grid, any fluctuations in the torque caused by wind variations are directly transferred to the generated electrical power, affecting system stability. For this reason, synchronous generators are not used in wind turbines that are directly connected to the grid but are instead utilized when interfaced with the grid through power converters, as shown in Figure.I.8 [Bri 13].

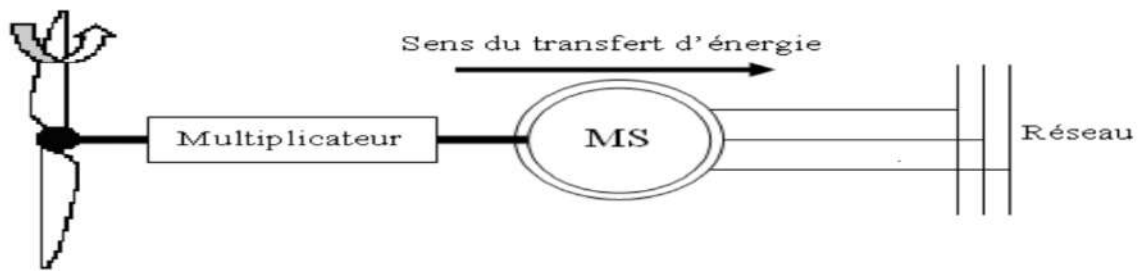


*Figure.I.8. Variable speed wind turbine based on the cage asynchronous machine.*

In this approach, the grid frequency is decoupled from the generator's rotational speed, allowing speed adjustments to maximize the wind turbine's aerodynamic efficiency and minimize torque fluctuations in the power transmission system. Some types of synchronous generators can operate at low speeds, enabling direct coupling with the turbine without the need for a gearbox, a common component in most wind turbines that requires frequent maintenance.

### **I.8.2. Asynchronous generator**

This type of generator offers greater flexibility when directly connected to the electrical grid due to the variation in slip between the magnetic flux in the stator and the rotor's rotational speed. For this reason, most fixed-speed wind turbines rely on induction generators. These generators are classified into two main types: squirrel cage induction generators and induction generators [Mel 22].

### **I.8.3. Asynchronous squirrel cage machine**

Cage asynchronous electric machines are simple in design and inexpensive to manufacture. They are standardized, produced in large quantities, and available in various power ratings. They also require minimal maintenance and have a low failure rate. Their direct grid connection is smoother due to slip variation between the stator flux and rotor speed, which is why they are widely [Mel 22].

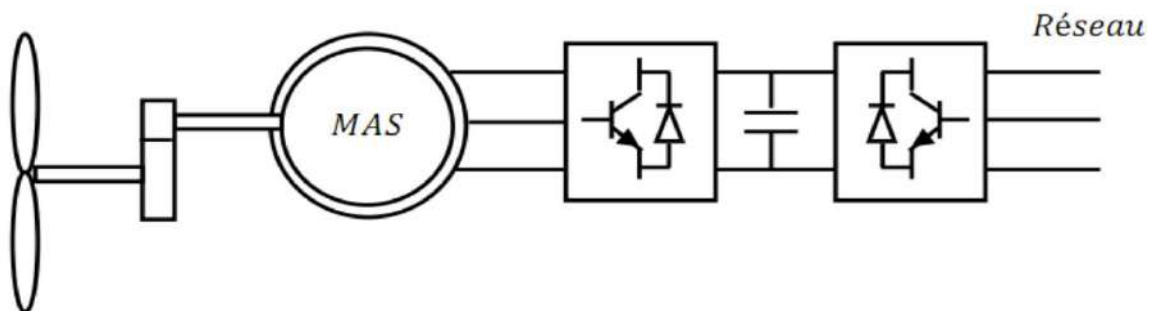


*Figure.I.9. Variable speed wind turbine based on the cage asynchronous machine.*

A squirrel cage induction generator (SCIG) can achieve variable-speed operation when connected to the grid via a power electronic converter. In this configuration, the capacitor bank is replaced with a full-scale converter, enabling speed variation regardless of wind conditions, as shown in Figure.I.10. Siemens has adopted this approach in its Bonus 107-3.6 MW model available on the market.

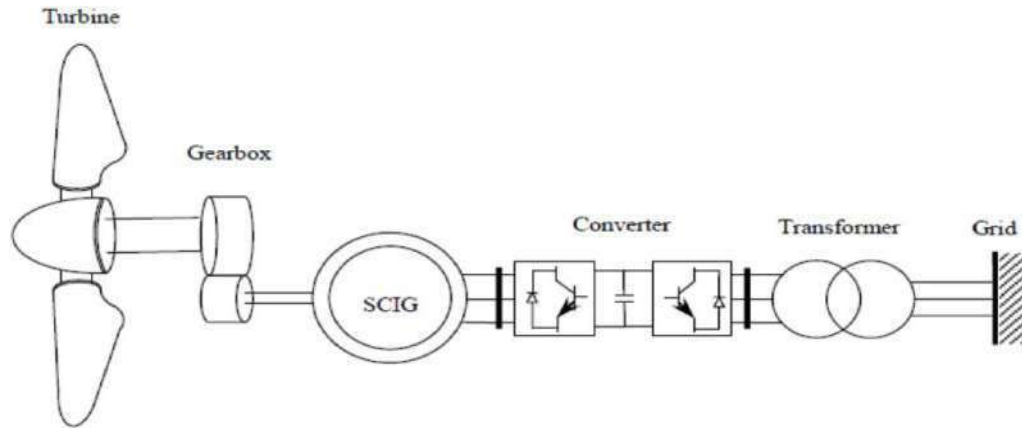


Figure.I.10. Multiple-stage geared SCIG concept with full-scale converter.

#### I.8.4. Double-fed asynchronous machine of the "wound rotor"

Along with synchronous generators, this type is one of the two leading solutions for variable-speed wind power. The stator is typically connected to the grid through a transformer. Unlike squirrel cage rotors, these machines feature a wound rotor, allowing slip variation through electrical control. Today, most wind projects above 1MW use rotor-driven asynchronous machines, where the stator is directly linked to the grid, and the rotor is connected via power converters [Mel 22], [Sad 20].

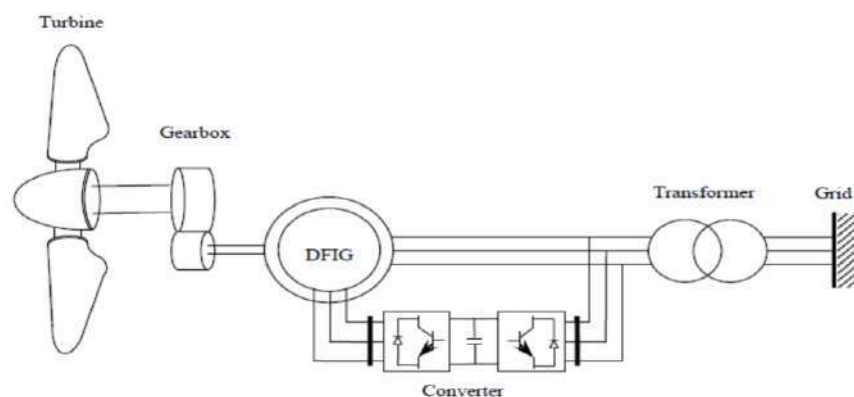


Figure.I.11. Variable speed concept with DFIG.

## **I.8.5. Permanent Magnetic Synchronous Generator System**

The permanent magnet synchronous generator (PMSG) is a suitable option for variable-speed systems when connected to the grid via a full-scale power converter. This converter adjusts the generator's variable-frequency voltage to match the grid frequency.

In recent years, the use of PMSG has become more attractive due to improvements in permanent magnet (PM) performance and a decrease in their cost.

Advantages of PMSG:

- Higher efficiency and greater energy output.
- No need for an additional power source for magnetic field excitation.
- Reduced field losses.
- Lower mechanical losses due to the absence of slip rings.
- Lighter weight, leading to a higher power-to-weight ratio.

Disadvantages of PMSG:

- High cost of permanent magnet materials.
- Complex manufacturing process.
- Risk of demagnetization at high temperatures.

PM machines offer flexible designs as they are not standardized, allowing for various configurations. Based on the direction of magnetic flux, they can be categorized into three types: radial flux, axial flux, and transverse flux machines [Bel 14].

## **I.9. Advantages and Disadvantages of Wind Turbines**

### **I.9.1. Advantages of Wind Turbine**

- Renewable Energy Source: Wind energy is inexhaustible and sustainable.
- Environmentally Friendly: No carbon emissions or pollutants are produced during operation.
- Low Operating and Maintenance Costs: Once installed, wind turbines require minimal maintenance compared to conventional energy sources.
- Suitable for Remote Areas: Can be used in locations far from main power grids.
- Technological Advancements: Continuous improvements in turbine technology increase efficiency and energy output.

- Energy Diversification: Helps reduce dependence on fossil fuels, enhancing energy security [Mel 22].

## I.9.2. Disadvantages of Wind Turbine

- Dependence on Wind Speed: Efficiency decreases when wind speeds are low, leading to fluctuations in power generation.
- High Initial Cost: Manufacturing and installation require significant investment.
- Visual and Noise Impact: Large turbines can be considered intrusive and produce noise during operation.
- Environmental Risks: May pose a threat to birds and wildlife in the installation areas.
- Space Requirements: Requires large open areas, which may not be feasible in urban settings.
- Grid Stability Issues: Fluctuating power generation may require integration with other energy sources to ensure a stable electricity supply [Szl 17].

## I.10. The Permanent Magnet Synchronous Machines (PMSM)

A **synchronous machine** refers to all machines in which the rotor rotates at the same speed as the magnetic field generated in the stator. To ensure this synchronization, the rotor's magnetic field is generated either using permanent magnets or through an excitation circuit. In this case, the rotor's magnetic field remains fixed relative to it, enforcing the alignment between the rotating magnetic field in the stator and the rotor's speed, hence the name **synchronous machine**.

The speed of rotation of the rotating field is proportional to the number of poles of the machine and the pulsation of stator currents. We note:

$$\omega_r = \omega / p$$

- The **stator** is the non-moving part of the electrical machine, where the windings connected to the power source are located. It is similar to the stator in all three-phase electrical machines. It consists of stacked magnetic metal sheets with slots, where three identical windings are placed, each offset by  $2\pi/3$  radians from the others [Ben 22].
- The rotor is the moving part of the machine and consists of permanent magnets. These magnets offer several advantages, such as eliminating the need for brushes, which reduces rotor losses. However, one drawback is that the rotor's magnetic flux cannot be controlled.

The rotor has different configurations. Figure (I.12) shows three typical cases for a four-pole rotor:

- **Figure (a)** illustrates a configuration of a **salient pole rotor**, where the pole pieces help concentrate the magnetic flux. In this design, the permanent magnets are magnetized in the **radial direction**.
- Another rotor configuration involves arranging the permanent magnets **radially**, embedding them within the rotor. In this case, the magnets are **tangentially magnetized**, as shown in **Figure (b)**.
- Finally, **Figure (c)** shows a configuration where the permanent magnets are evenly distributed on the cylindrical surface of the rotor. In this case, the magnets are radially magnetized.

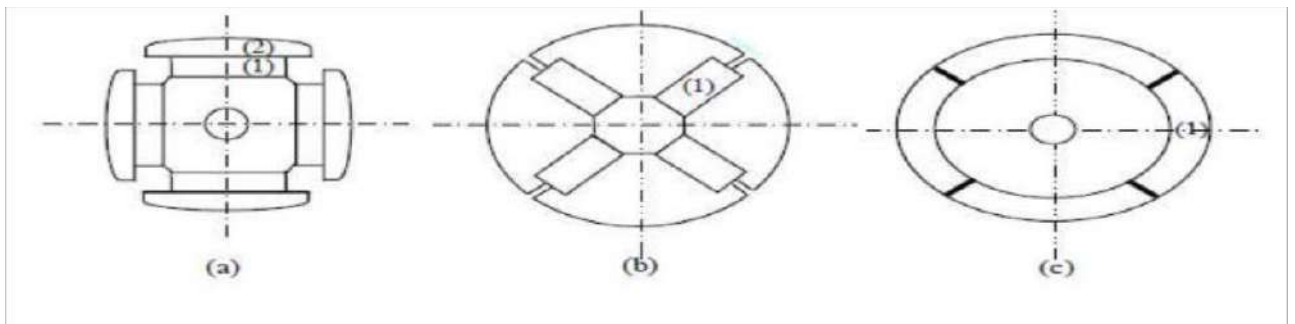


Figure I.12. different types of rotor of an (PMSMs).

### I.10.1. Operating principle (PMSM)

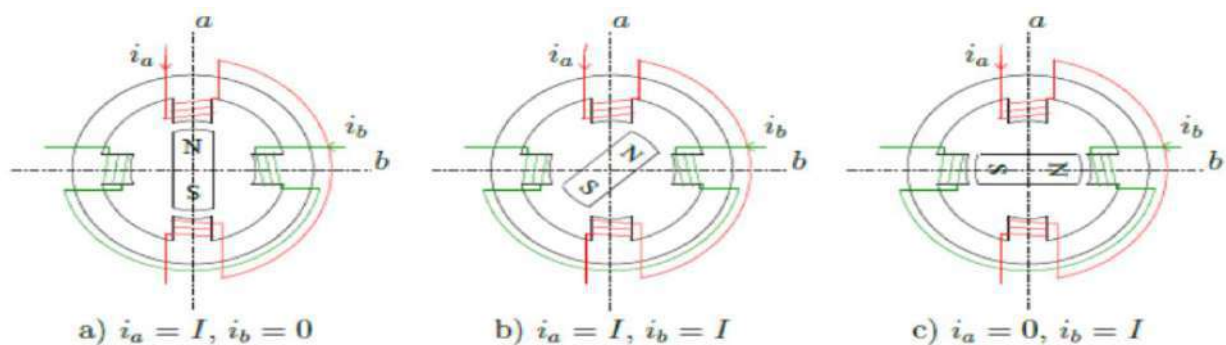


Figure I.13. Operating principle of the permanent magnet motor.

The principle of permanent magnet motors is quite simple. Only the coils are powered. The field created by the windings orients the rotor which is made up of magnets. Figure (I.2) represents a motor having a bipolar rotor and a stator comprising a pair of poles. Phases a and b

are carried by opposite windings. The presence of currents in the phases directs the rotor. We define an elementary “step”  $\theta_p$  as being the angular displacement of the rotor when the power supply is switched from one phase to the next. We obtain for this structure  $\theta_p=90^\circ$ . This corresponds to the passage in Figure(I.13.a) in Figure (I.13.c). Half-steps are obtained by powering two phases at the same time Figure (I.13.b). This type of structure is widely used in many motors on the market [All 17].

### **I.10.2. Torque of permanent magnet synchronous machines**

There are three types of couple [All 17]:

- **Torque relaxing**

When the magnets rotate with the rotor and pass in front of the stator teeth, they encounter a variation in magnetic reluctance, generating a torque with a zero average value, known as detent torque. To mitigate this effect, the stator slots can be inclined by one slot pitch, but this complicates the winding process. A more advantageous solution is to tilt the rotor magnets, as this approach effectively reduces detent torque while simplifying the winding manufacturing process.

- **Reluctance couple**

Also known as saliency torque, it occurs due to variations in the inductance of the stator windings depending on the rotor position. It is important to note that in the case of surface-mounted magnets, the armature flux encounters a constant reluctance regardless of the rotor's position. As a result, reluctance torque is not present in these types of motors.

- **Mutual couple**

It is due to the interaction of the two stator and rotor fields.

## **I.11. Advantages of Permanent Magnet Synchronous Machines (PMSM)**

Permanent Magnet Synchronous Machines (PMSM) offer several advantages compared to machines that use excitation windings. The key benefits include [All 17]:

- Elimination of rotor power supply, avoiding the need for slip rings and brushes.
- Reduction in copper losses, as most losses occur in the stator.
- Improved power factor and higher motor efficiency.

- Low inertia and high torque-to-mass ratio.
- Superior dynamic performance, enhancing system responsiveness.
- Simplified construction and maintenance.
- No rotor heating and elimination of Joule losses.

## **I.12. Disadvantages of Permanent Magnet Synchronous Machines (PMSM)**

Despite the numerous advantages of Permanent Magnet Synchronous Machines (PMSM), they have some limitations, including [Ben 22]:

- Complex and costly control, Replacing the mechanical switch with an advanced electronic control system makes motor operation more complicated and expensive compared to DC motors.
- High cost, due to the expensive permanent magnets, which affects the economic feasibility of this technology.
- Torque ripple, which can impact operational stability and control precision.
- Risk of demagnetization, imposing strict operating constraints, such as maximum temperature and current limits.
- Eddy current losses in the magnets, which can reduce energy efficiency and cause unwanted heating of the motor.

## **I.13. Applications of (PMSM) in renewable energy systems**

Permanent Magnet Synchronous Machines (PMSMs) are widely used in renewable energy systems, playing a crucial role in efficient electricity generation. In wind turbines, PMSMs function as generators that convert the mechanical energy from rotating blades into electrical energy, enhancing wind power generation efficiency. Similarly, these machines are used in hydroelectric power plants, where they convert the energy of flowing water into electricity, contributing to the sustainable application of water resources. PMSMs in renewable energy systems are characterized by their high efficiency and power density, enabling greater energy production with minimal losses. Moreover, help decrease environmental impact and improve sustainability of energy sources.

These machines are employed in a wide range of applications across various fields, such as household appliances, CD/DVD players, computer hard drives, electric cars and bicycles, transportation, aerospace, manufacturing machines, servo motors, medical equipment, and ship

propulsion. They cover power microwatts to megawatts. Figure (I.14) shows some applications of these machines [Bou 12],[Mel 22],[Aya 17].

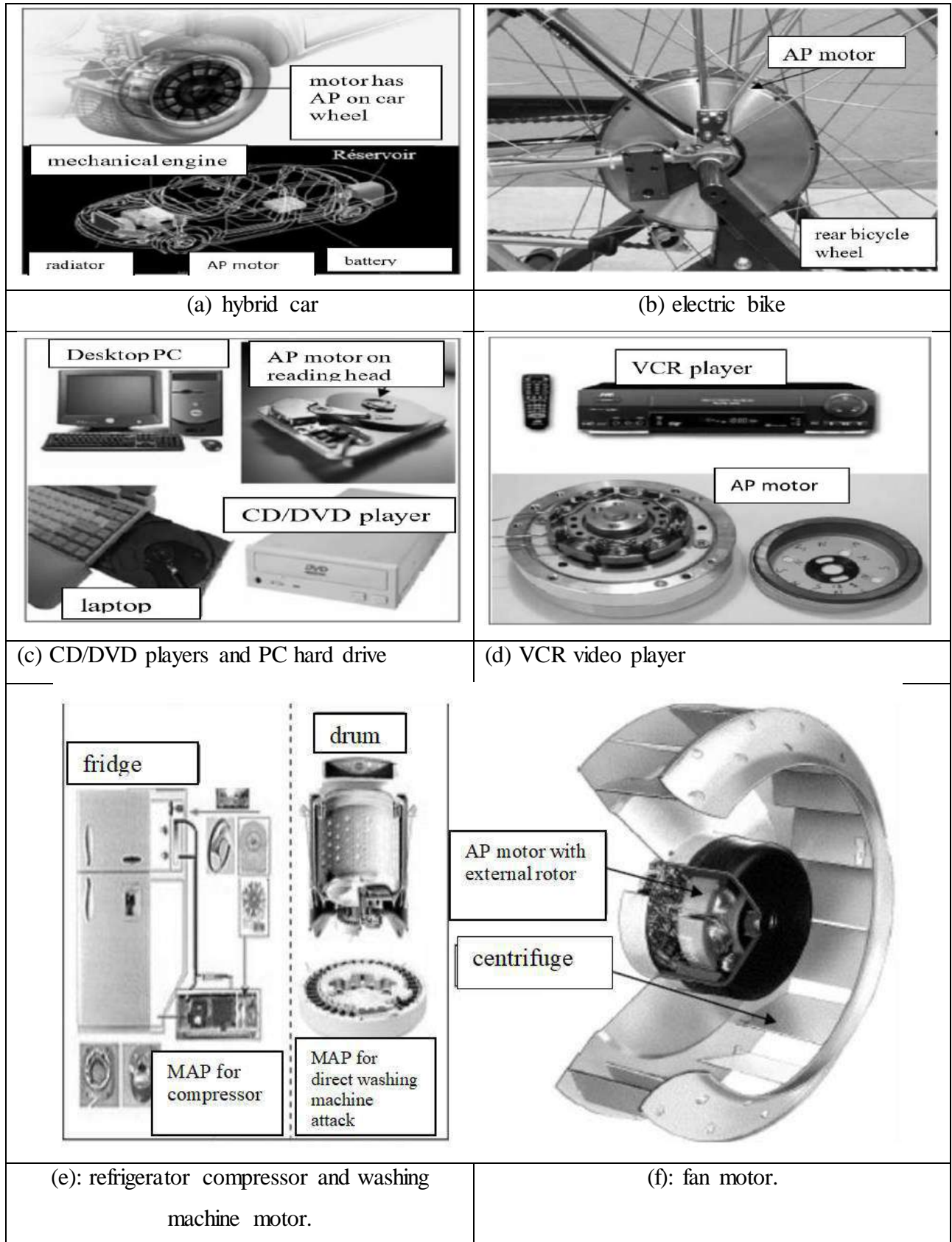


*Figure .I.14. Applications principle of Permanent Magnet Synchronous Machines (PMSM).*

## **I.15. Conclusion**

In conclusion, wind turbines and Permanent Magnet Synchronous Machines (PMSMs) are among the most effective technologies in the field of renewable energy, providing a clean and sustainable source of electricity with high efficiency and reliability. PMSMs units operate the performance of wind turbines by efficiently converting mechanical energy into electrical energy, reducing energy losses and promoting sustainability. With ongoing technological advancements, these technologies will remain fundamental to achieving a cleaner and more.

In this chapter, we provided a general concept, working principle, components, and discussed wind resources of wind turbine, different wind energy conversion systems, the applications of wind turbine converters, and the configurations of variable-speed WECS, highlighting the advantages and disadvantages of wind turbines.

Furthermore, we explored the structure of the permanent magnet synchronous machine (PMSM), explaining its working principle and torque, as well as its applications in renewable energy. Additionally, we highlighted its various advantages and disadvantages.

# **Chapter II: Modeling of Wind Energy System Components**

## II.1. Introduction

The Permanent Magnet Synchronous Machine (PMSMs) are widely used due to their high efficiency and fast dynamics, mainly resulting from the use of permanent magnets on the rotor, which eliminates the need for external excitation and reduces energy losses. Accurate dynamic modeling of the PMSM is essential for designing effective control strategies. Typically, the machine is modeled in the rotating dq-reference frame, which decouples the torque and flux components, thus resembling the behavior of a separately excited DC machine and simplifying control implementation.

In this context, the present study aims to develop a mathematical model of the PMSM to serve as a foundation for applying advanced control techniques such as Field-Oriented Control (FOC) and Model Predictive Control (MPC) in later chapters.

## II.2. Modeling of the permanent magnet synchronous machine

The formulation of a mathematical model for a Permanent Magnet Synchronous Machine (PMSM) is essential for studying its control under various operating conditions, both transient and steady-state [Ben05].

The commonly adopted simplifying assumptions in the modeling of the machine, as found in most references, are as follows [Yah 05]:

- Constant winding resistance (independent of temperature);
- Negligible skin effect,
- Absence of magnetic circuit saturation,
- The machine is supplied by a system of balanced, sinusoidal three-phase voltages,
- Perfect structural symmetry,
- Sinusoidal spatial distribution of magneto motive forces along the air gap,
- Uniform air gap thickness and negligible slotting effect,
- Negligible iron losses (due to hysteresis and eddy currents).

These assumptions imply that both the electrical and magnetic behaviors are considered linear.

### II.1.1 Equation of the PMSM model

Figure (II.1) shows the representation of the windings for a three-phase permanent magnet synchronous machine:

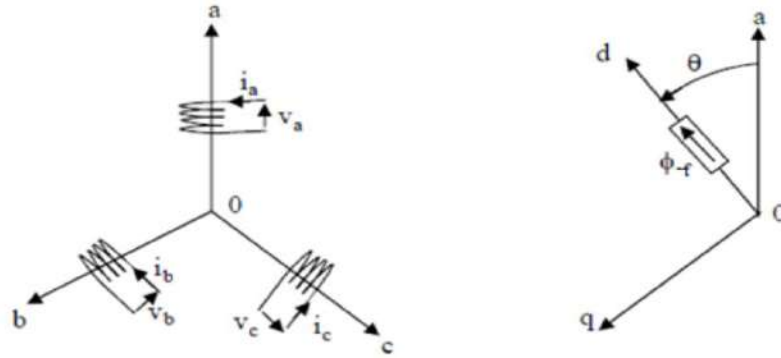


Figure II.1. Representation of a permanent magnet synchronous machine.

The mathematical model of the PMSM is comparable to that of the classical synchronous machine [Kad 00],[Cha 06]. The machine's equations are written as follows for an equilibrated machine:

Electrical equations:

$$[V_{abc}]_s = [R_S][i_{abc}]_s + \frac{d}{dt} [\varphi_{abc}]_s$$

(II.1)

Magnetic equations:

$$[\varphi_{abc}]_s = [L_S][i_{abc}]_s + [\varphi_{f,abc}]$$

(II.2)

OR:

$[V_{abc}]_s = [V_a \ V_b \ V_c]^T$  : Stator voltage vector;

$[i_{abc}]_s = [i_a \ i_b \ i_c]^T$  : Stator current vector;

$[\varphi_{abc}]_s = [\varphi_a \ \varphi_b \ \varphi_c]^T$  : Stator flux vector;

$$[R_S] = \begin{bmatrix} R_S & 0 & 0 \\ 0 & R_S & 0 \\ 0 & 0 & R_S \end{bmatrix} : \text{Stator resistance matrix};$$

$[\varphi_{f,abc}] = [\varphi_{af} \ \varphi_{bf} \ \varphi_{cf}]^T$  : Flux vector created by the magnet through the stator winding.

We define:

$[L_S]$ : Stator inductance matrix. It contains constant terms that we group in  $[L_{S0}]$  and variable terms depending on  $\theta$ , which we group in  $[L_{S2}(\theta)]$ :

$$[L_S] = [L_{S0}] + [L_{S2}] \quad (II.3)$$

$$[L_{S0}] = \begin{bmatrix} L_{S0} & M_{S0} & M_{S0} \\ M_{S0} & L_{S0} & M_{S0} \\ M_{S0} & M_{S0} & L_{S0} \end{bmatrix}; [L_{S2}] = L_{S2} \begin{bmatrix} \cos(2\theta) & \cos 2\left(\theta - \frac{2\pi}{3}\right) & \cos 2\left(\theta - \frac{4\pi}{3}\right) \\ \cos 2\left(\theta - \frac{2\pi}{3}\right) & \cos 2\left(\theta - \frac{4\pi}{3}\right) & \cos(2\theta) \\ \cos 2\left(\theta - \frac{4\pi}{3}\right) & \cos(2\theta) & \cos 2\left(\theta - \frac{2\pi}{3}\right) \end{bmatrix}$$

Where:

$M_{S0}$ : mutual inductance between two stator phases,

$L_{S0}$ : self-inductance of a stator phase,

$\theta$ : characterizes the angular position of the rotor relative to the stator.

The fundamental mechanical equation describing the rotor dynamics represents the final key relation that completes the model of the PMSM.

$$J \frac{d\Omega}{dt} + f_r \Omega = T_e - T_r \quad (\text{II.4})$$

With:

- $J$ : Moment of inertia of the rotating part;
- $\Omega$ : Mechanical angular velocity of the rotor;
- $T_e$ : Electromagnetic torque of the machine;
- $T_r$ : Resistant or load torque;
- $f_r$ : Coefficient of friction.

## II.1.2 Machine equation in the Park frame (d, q)

The equations obtained in the (a,b,c) reference frame are highly nonlinear and coupled, and they depend on the rotor position  $\theta$ . This complicates the control strategy due to the dependence on rotor position. To simplify this issue, most of the studies in the literature rely on the use of the Park transformation. When applied to the real variables (voltages, currents, and fluxes), this transformation converts them into fictitious variables known as the d-q or Park components. This can be interpreted as substituting the windings of the real system phases (a, b, c) with orthogonal (d, q) axis windings rotating at a speed  $\omega$  relative to the stator (see Figure II.2). This change of reference frame simplifies the machine's dynamic equations, making their study and analysis easier [Nai 07].

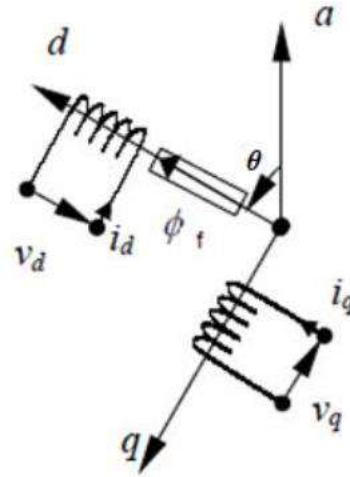


Figure.II.2. Equivalent representation in the Park frame.

The Park transform is defined as follows:

$$[X_{dqo}] = [P(\theta)][X_{abc}] \quad (\text{II.5})$$

where  $\theta$  denotes the rotor's position and  $X$  could be a current, tension, or flux. the statoric variables (tensions, currents, fluxes, and inductances) are represented by the terms  $X_d$  and  $X_q$ .

The transformation matrix  $[P(\theta)]$  is given by:

$$[P(\theta)] = \frac{2}{3} \begin{bmatrix} \cos(\theta) & \cos\left(\theta + \frac{2\pi}{3}\right) & \cos\left(\theta + \frac{4\pi}{3}\right) \\ -\sin(\theta) & -\sin\left(\theta + \frac{2\pi}{3}\right) & -\sin\left(\theta + \frac{4\pi}{3}\right) \\ 1/2 & 1/2 & 1/2 \end{bmatrix} \quad (\text{II.6})$$

Where  $\theta$  corresponds to the position of the coordinate system chosen for the transformation.

the inverse matrix is given by:

$$[P(\theta)]^{-1} = \begin{bmatrix} \cos(\theta) & -\sin(\theta) & 1 \\ \cos\left(\theta + \frac{2\pi}{3}\right) & -\sin\left(\theta + \frac{2\pi}{3}\right) & 1 \\ \cos\left(\theta + \frac{4\pi}{3}\right) & -\sin\left(\theta + \frac{4\pi}{3}\right) & 1 \end{bmatrix} \quad (\text{II.7})$$

With  $\theta = \theta_s$  for the stator and  $\theta = \theta_r$  for the rotor.

Since the motor is connected in a star (wye) configuration, it forms a balanced system, such that  $I_a + I_b + I_c = 0$ . Consequently, the zero-sequence (homopolar) component, represented by the third row of matrix (II.6), is null.

### II.1.3 Transition from the d q frame to the $\alpha \beta$ frame

The transition to Park components is given by a rotation matrix [Bou 06]:

$$[X_{\alpha\beta}] = [R][X_{dq}] \quad (\text{II.8})$$

With :

$$[R] = \begin{bmatrix} \cos \theta & -\sin \theta \\ \sin \theta & \cos \theta \end{bmatrix} \quad (\text{II. 9})$$

### II.1.4 Application of the Park transformation to PMSM

Choosing the Park frame (d, q) linked to the rotor and applying the transformation (II.5) to the system (II. 1), we obtain:

$$[V_{dq}] = [P(\theta)][V_{abc}]_s = [P(\theta)][R_S][i_{abc}]_s + [P(\theta)] \frac{d}{dt} [\varphi_{abc}]_s \quad (\text{II.10})$$

Then, based on (II.7) and (II.1) we obtain:

$$[V_{dq}] = [P(\theta)][R_S][P(\theta)]^{-1}[i_{dq}] + [P(\theta)][P(\theta)]^{-1} \frac{d}{dt} [\varphi_{dq}] + [P(\theta)] \left( \frac{d}{dt} [P(\theta)]^{-1} \right) [\varphi_{dq}] \quad (\text{II.11})$$

Du moment que  $[R_S]$  est diagonale, alors :

$$[P(\theta)][R_S][P(\theta)]^{-1} = [R_S]$$

Using:

$$[P(\theta)] \left( \frac{d}{dt} [P(\theta)]^{-1} \right) = \frac{d\theta}{dt} \begin{bmatrix} 0 & -1 & 0 \\ 1 & 0 & 0 \\ 0 & 0 & 0 \end{bmatrix} \quad (\text{II.12})$$

And using (II.11), we can deduce the Park equations in vector form as follows:

$$[V_{dq}] = [R_S][i_{dq}] + \frac{d}{dt} [\varphi_{dq}] + p\Omega[\varphi_{dq}^*] \quad (\text{II.13})$$

Or :

$$[V_{dq}] = \begin{bmatrix} V_d \\ V_q \end{bmatrix}; [R_S] = \begin{bmatrix} R_S & 0 \\ 0 & R_S \end{bmatrix}; [i_{dq}] = \begin{bmatrix} i_d \\ i_q \end{bmatrix}$$

$$[\varphi_{dq}] = \begin{bmatrix} \varphi_d \\ \varphi_q \end{bmatrix}; [\varphi_{dq}^*] = \begin{bmatrix} -\varphi_q \\ \varphi_d \end{bmatrix}$$

And the transformation (II.6) applied to (II.2) gives:

$$\begin{bmatrix} \varphi_d \\ \varphi_q \end{bmatrix} = \begin{bmatrix} L_d & 0 \\ 0 & L_q \end{bmatrix} \begin{bmatrix} i_d \\ i_q \end{bmatrix} + \begin{bmatrix} \varphi_f \\ 0 \end{bmatrix} \quad (\text{II.14})$$

## II.2 Expression of the electromagnetic torque

The electromagnetic torque  $C_e$  results from the interaction between the magnetic poles of the rotor, created by the permanent magnets, and those generated in the air gap by the magnetomotive forces (MMF) induced by the stator currents [Guy 00]. In the case of synchronous machines with sinusoidal electromotive force (e.m.f.) and without damper windings, this torque can be expressed by the following relation:

$$T_e = \left(\frac{m}{2}\right)p[(L_d - L_q)i_d i_q + \varphi_f i_q] \quad (II.15)$$

Or :

$p$ : number of pole pairs.  $m$ : number of phases of the machine.

In the case of a smooth-pole machine ( $L_d = L_q$ ), this equation simplifies to:

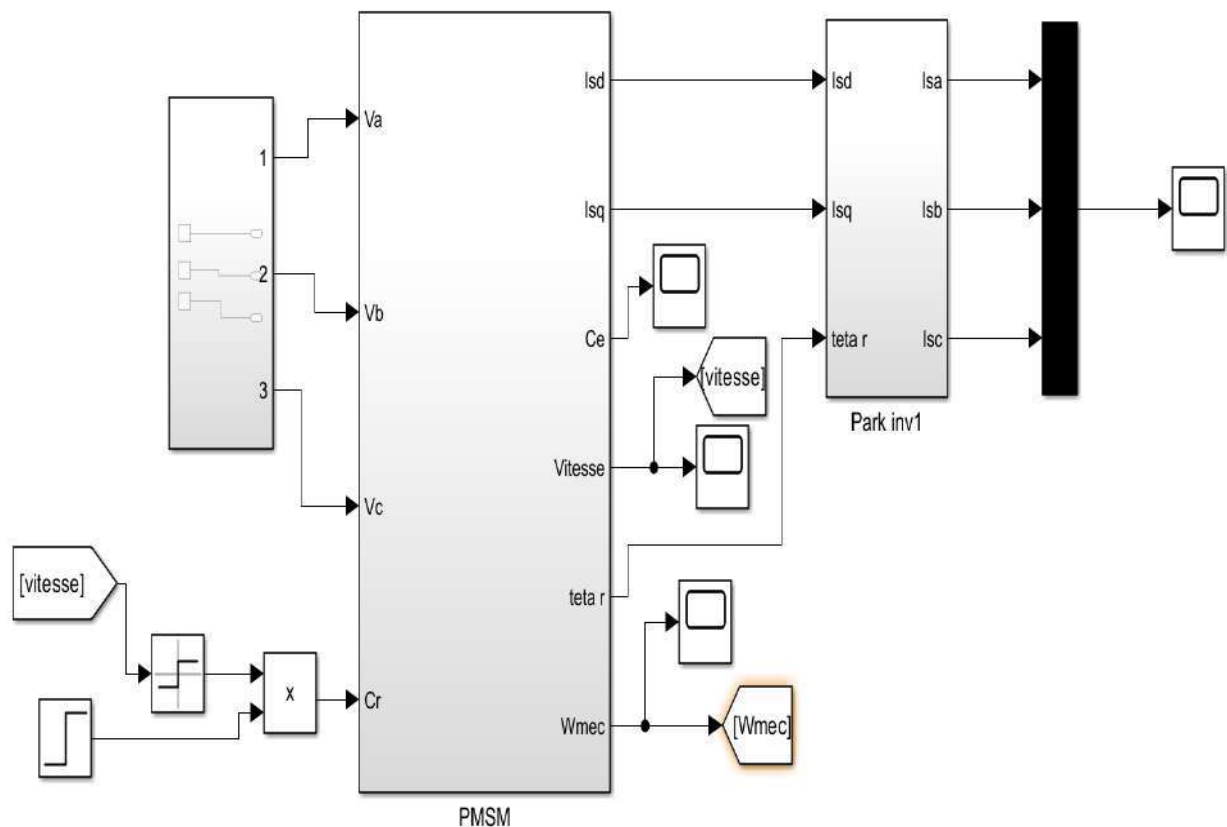
$$T_e = \left(\frac{m}{2}\right)p\varphi_f i_q \quad (II.16)$$

### II.3 Formation of state equation

Let us consider the voltages ( $V_d, V_q$ ) as control variables, and the stator currents ( $i_d, i_q$ ) as state variables. From equations (II.13), (II.14), we can write the system of equations as follows:

$$\frac{d}{dt} \begin{bmatrix} i_d \\ i_q \end{bmatrix} = \begin{bmatrix} -\frac{R_s}{L_d} & \frac{L_q}{L_d} p\Omega \\ \frac{L_d}{L_q} p\Omega & -\frac{R_s}{L_d} \end{bmatrix} \begin{bmatrix} i_d \\ i_q \end{bmatrix} + \begin{bmatrix} \frac{1}{L_d} & 0 \\ 0 & \frac{1}{L_q} \end{bmatrix} \begin{bmatrix} V_d \\ V_q \end{bmatrix} + \begin{bmatrix} 0 \\ -\frac{p\Omega}{L_q} \end{bmatrix} [\varphi_f] \quad (II.17)$$

### II.4 Modeling of PMSM by MATLAB/Simulink



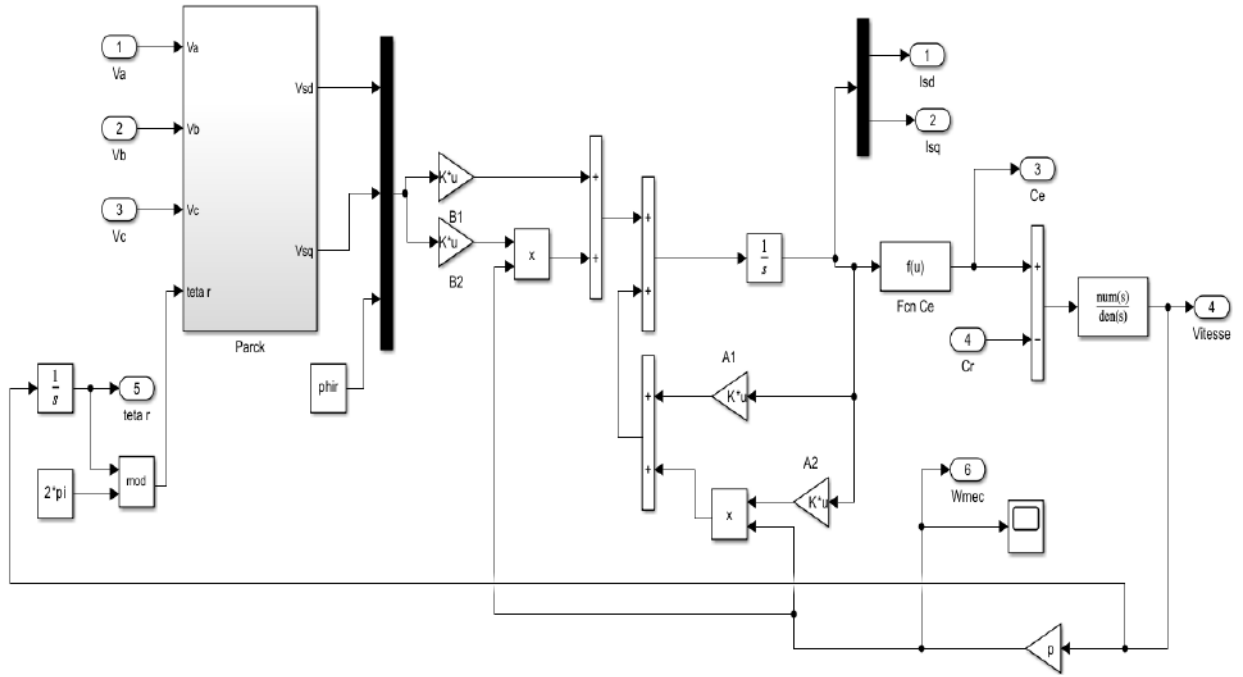


Figure.II.3. Modeling of PMSM by MATLAB/Simulink.

## II.5 Modeling of the Wind Turbine

In this chapter, we focus exclusively on the modeling of a horizontal-axis three-blade wind turbine, as shown in Figure II.21. All models have been developed for implementation in MATLAB/SIMULINK, which allows for the rapid setup of models as well as their associated control laws. This environment is well-suited for simulating the mechanical and electromechanical phenomena studied here [CAB 03].

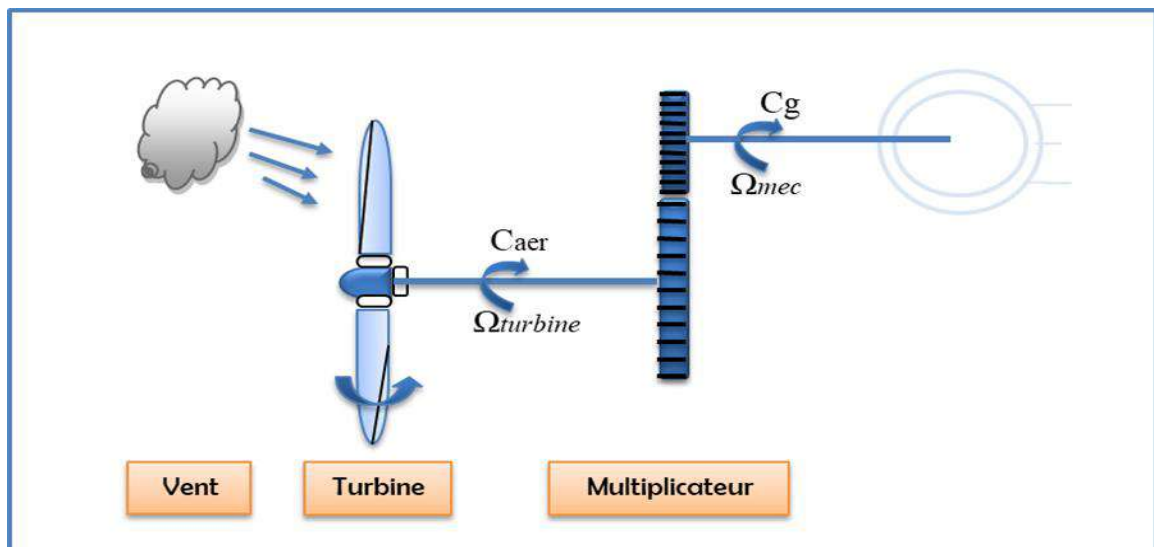


Figure.II.4. Schéma de la turbine éolienne.

## II.5.1 Wind Modeling

Wind resource, in terms of its statistical distribution, is essential in a wind energy project and is therefore a key factor in calculating electricity production and profitability. The dynamic properties of wind are crucial for studying the entire energy conversion system, as wind power, under optimal conditions, is proportional to the cube of the wind speed.

Wind speed is a three-dimensional vector. However, the vertical component of the wind speed vector is not significant from the perspective of the wind turbine, as it does not interact with its active surface. For simplification purposes, the wind speed vector is considered to evolve in the horizontal plane.

Horizontal-axis wind turbines lack any blade orientation mechanism (the active surface always faces the wind), which allows for a significant simplification of the wind behavioral model. Therefore, wind speed can be modeled as a scalar function that evolves over time:

$$v(t) = f(t) \quad (\text{II.18})$$

In a deterministic form as a sum of several harmonics:

$$v(t) = A + \sum_{n=1}^i (a_n \cdot \sin(b_n \cdot \omega_v \cdot t)) \quad (\text{II.19})$$

We will use the following wind equation as an example in our modeling:

$$v(t) = 6.5 + 0.02\sin(0.1047t) + 0.2\sin(0.2665t) + 0.1\sin(1.2930t) + 0.02\sin(3.6645t) \quad (\text{II.20})$$

## II.5.2 Modeling of a Horizontal-Axis Wind Turbine

The wind turbine captures the kinetic energy of the wind and converts it into torque that rotates the rotor blades. Three factors determine the ratio between the wind's energy and the mechanical energy recovered by the rotor : Air density, the swept area of the rotor, and wind speed. Air density and wind speed are climatological parameters that depend on the specific site [KEN 12].

The turbine model consists of three blades of length R, driving a generator through a gearbox with a gain G, as shown in Figure II.20 [ELA 04] [GHE 11].

This results in a global model composed of three subsystems:

- The turbine
- The multiplicateur
- arbre

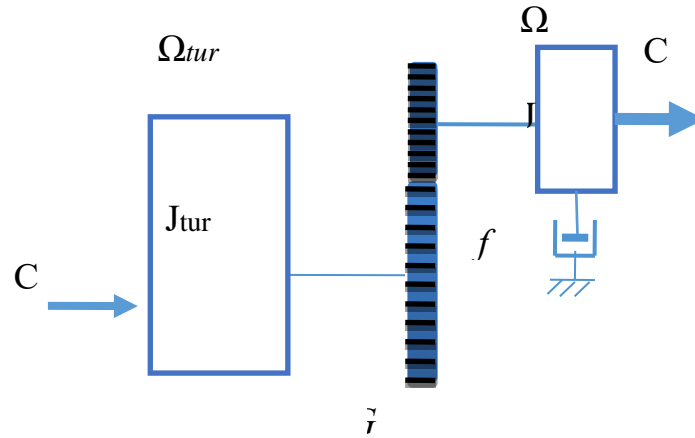


Figure.II.5. Simplified mechanical model of the turbine.

### II.5.2.1 Modeling of the turbine

Turbine modeling involves expressing the extractable power as a function of the incoming wind speed and the operating conditions—particularly the rotational speed. This makes it possible to determine the wind torque applied to the low-speed shaft of the wind turbine.

The wind power, or aerodynamic power, is defined as follows [SAG 98] [BEC 13]:

$$P_{vent} = \frac{1}{2} \rho S V_{vent}^3 = \frac{1}{2} \rho \cdot \pi \cdot R^2 \cdot V_{vent}^3 \quad (II.21)$$

$\rho$ : Is the air density, equal to 1.22 kg/m<sup>3</sup> at atmospheric pressure and 15°C. According to Betz's law, this power can never be fully extracted.

$S$ : Is the circular area swept by the turbine. The radius of this circle is determined by the blade length  $R$  où  $S = \pi R^2$ .

$V_{vent}$ : Is the wind speed.

In reality, the conversion device (the wind turbine) extracts an aerodynamic power  $P_{aer}$  which is lower than the available power  $P_v$ .

$$P_{aer} = \frac{1}{2} C_p(\lambda, \beta) \rho \pi R^2 V^3 \quad (II.22)$$

The wind turbine can only convert a certain percentage of the captured wind power [ELA 03]. This percentage is represented by  $C_p(\lambda, \beta)$  which depends on the tip speed ratio  $\lambda$  and the blade pitch angle  $\beta$ .

The power coefficient  $C_p$ , represents the aerodynamic efficiency of the wind turbine ( $\frac{P_{aer}}{P_v}$ ). It depends on the turbine's characteristics. The expression of the power coefficient is interpolated in the following form [ELA 04],[ABD 00]:

$$C_p(\beta, \lambda) = (0.5 - 0.0167 \cdot (\beta - 2)) \cdot \sin\left(\frac{\pi \cdot (\lambda + 0.1)}{18.5 - 0.3(\beta - 2)}\right) - 0.00184(\lambda - 3) \cdot (\beta - 2) \quad (II.23)$$

The actual power coefficient curve  $C_p$  of the wind turbine studied in this thesis is illustrated in Figure II.6. The maximum power coefficient is  $C_{p_{max}} = 0.5$  which corresponds to a blade pitch angle of  $\beta = 2^\circ$  and an optimal tip speed ratio of  $\lambda_{optim} = 9.2$ .

To extract the maximum generated power, the tip speed ratio  $\lambda_{optim}$  must be set to  $\lambda_{optim}$ , and the power coefficient should be maintained at its maximum value  $C_{p_{max}} = 0.5$ .

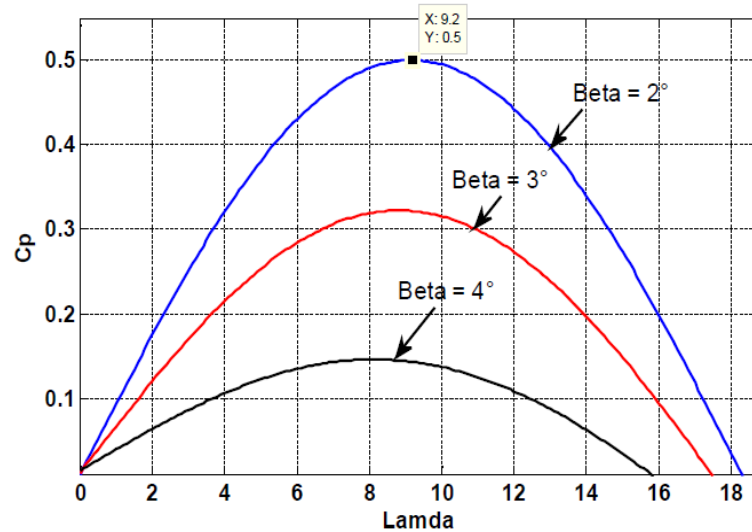


Figure II.6. Power coefficient  $C_p$  as a function of the tip speed ratio  $\lambda$

The blade pitch angle  $\beta$ .

The turbine torque is the ratio of the aerodynamic power to the rotational speed of the turbine  $\Omega_t$ :

$$C_t = \frac{P_{aer}}{\Omega_t} \quad (II.24)$$

$\Omega_t$ : Turbine speed;

$C_{aer}$ : Aerodynamic torque.

The tip speed ratio  $\lambda$  is defined as the ratio between the linear speed of the blades (the rotational speed of the turbine) and the wind speed. [ELA 04]:

$$\lambda = \frac{\Omega_t R}{v} \quad (II.25)$$

It can be observed from Figure II.16 that the power coefficient reaches a maximum at a specific value of the tip speed ratio, referred to as  $\lambda_{opt}$ . At this point, the power coefficient  $C_p$  is at its maximum, which consequently results in maximum captured power.

It is therefore possible to develop control laws that enable the capture of maximum power regardless of the wind speed, up to the rated power of the generator, beyond which the extracted power is limited to this nominal value [DAV 07].

### II.5.2.2 Multiplier Model

The multiplier adjusts the (low) speed of the turbine to the speed of the generator. The turbine is typically coupled to the generator shaft through a gearbox whose speed ratio  $G$  is selected to bring the generator shaft speed within a desired operating range. By neglecting transmission losses, the turbine's torque and speed are related to the generator side. This gearbox is mathematically modeled as a simple gain using the following equations:

$$C_g = \frac{C_{aer}}{G} \quad (II.26)$$

$$\Omega_{turbine} = \frac{\Omega_{mec}}{G} \quad (II.27)$$

Où :

$C_g$  : Multiplier torque;

$\Omega_{mec}$  : Is the rotational speed of the generator;

$G$  : Multiplier Gain.

### II.5.2.3 Dynamic Equation of the blade (arbre)

The mass of the wind turbine is transferred to the turbine shaft in the form of an inertia  $J_t$ , which accounts for the blades and the mass of the turbine rotor. The proposed mechanical model considers the total inertia  $J$ , which consists of the turbine's reflected inertia on the generator rotor and the inertia of the generator itself [GHE 11] [ABD 13].

$$J_t = J_g + J_t G^2 \quad (II.28)$$

$$C_{mec} = J_t \frac{d\Omega}{dt} \quad (II.29)$$

The mechanical equation governing such a system is given by :

$$C_{mec} = C_g - C_{em} - C_{vis} \quad (II.30)$$

$$C_g - C_{em} = J_t \frac{d\Omega_{mec}}{dt} + f\Omega_{mec} \quad (II.31)$$

Where :

$J_t$ : It is the total inertia that appears on the generator rotor;

$C_{em}$  : Is the electromagnetic torque;

$C_{vis}$  : Le couple de frottement visqueux.

The block diagram corresponding to the wind turbine modeling is easily derived from the above equations and is shown in Figure II.24.

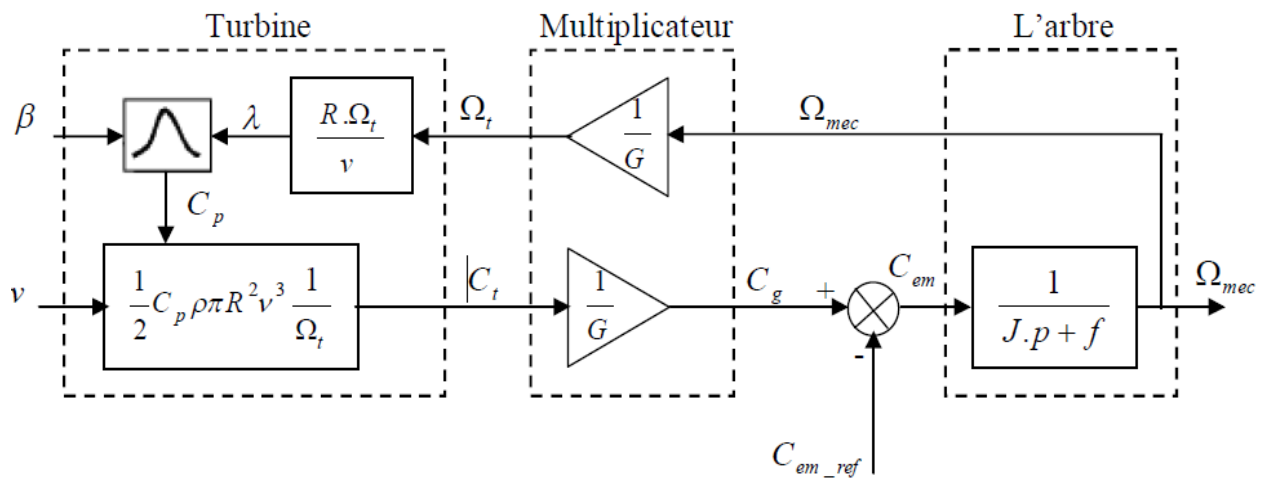


Figure.II.7. Block diagram of the wind turbine model.

## II.6 Wind Turbine Model in MATLAB/SIMULINK

The turbine model is easily derived from the above equations and is illustrated in Figure II.8.

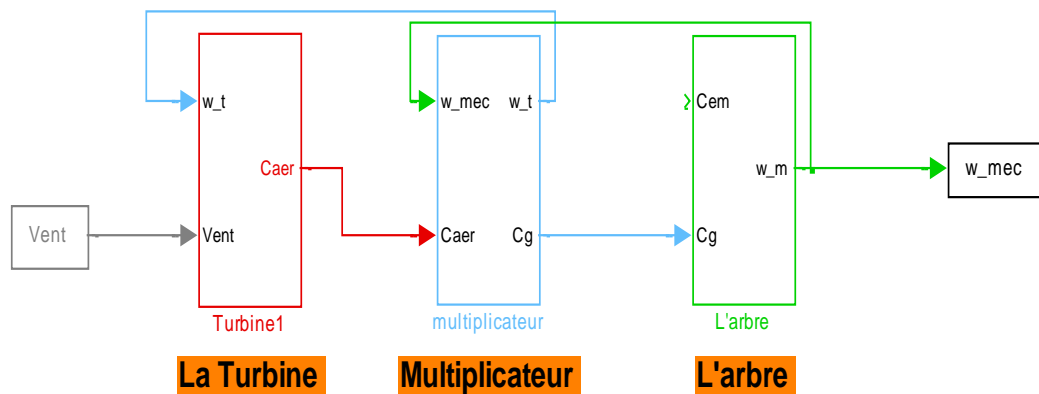


Figure.II.8. Block model of the wind turbine .

The turbine generates an aerodynamic torque that is transmitted to the multiplicator. This torque can be calculated from the wind speed and the turbine's rotational speed.

The multiplicator converts the turbine speed and aerodynamic torque into mechanical speed and torque at its output.

The turbine can thus be controlled through the action of the electromagnetic torque from the electrical converter. The wind speed is considered as a disturbance.

## II.7 Modeling of a PWM Voltage Rectifier

The three-phase PWM rectifier consists of three legs. The bidirectionally controlled switches with two segments are fully controllable switches (both turn-on and turn-off), replacing the diodes used in the conventional Graetz bridge configuration [NOU 04].

These devices offer the following advantages:

- The current and voltage can be modulated (Pulse Width Modulation or PWM), which results in lower harmonic disturbances.
- The power factor can be controlled.
- The rectifier (redresseur) can be considered either as a voltage source or a current source [KOR 09].

The topology of a three-phase voltage PWM rectifier is shown in Figure II.9. Each switch consists of a bidirectionally controlled power semiconductor device and an anti-parallel diode. This switch is unidirectional in voltage and bidirectional in current. Therefore, due to its structure, this converter is current-reversible.

Unlike conventional rectifiers, PWM rectifiers are built using controlled semiconductor devices. The ability to control both turn-on and turn-off enables full control of the converter, as the switches can be operated as needed in both directions at relatively high switching frequencies [BOU 10].

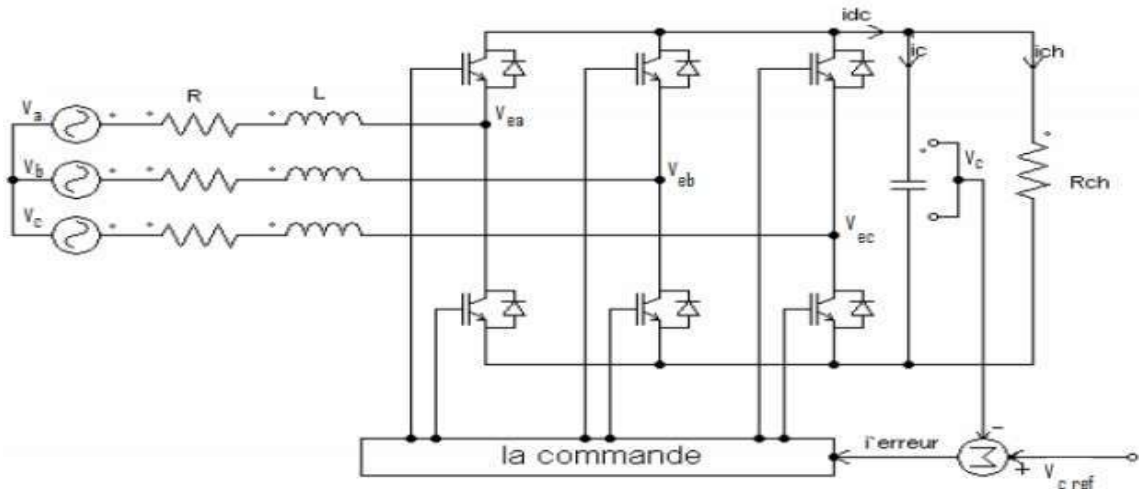


Figure.II.9. Basic Topologies of a Voltage Rectifier.

## II.7.1 Operating principle of a PWM rectifier MLI

The voltage rectifier operates by maintaining the DC bus voltage at a desired reference value using closed-loop control, as shown in Figure III.10. To accomplish this, the DC bus voltage  $V_{dc-ref}$  is measured and compared to a reference  $V_{dc}$ . The error signal resulting from this comparison is used to switch the six rectifier switches on and off.

In this way, power can flow in both directions depending on the conditions of the measured DC bus voltage  $V_{dc}$  across the capacitor C.

When the current  $i_{ch}$  is positive (rectifier operation), the capacitor C is discharged, and the error signal instructs the control block to draw more power from the AC source. The control block takes power from the AC source by generating an appropriate PWM signal for the six switches. In this way, more current flows from the AC source to the DC side, and the capacitor voltage is restored.

Conversely, when  $i_{ch}$  becomes negative (inverter operation), the capacitor C is overloaded, and the error signal instructs the control block to discharge the capacitor, returning power to the AC source.

PWM control not only can control active power, but also reactive power, this type of rectifier allows power factor correction. In addition, the waveforms of the source currents can be maintained as almost sinusoidal, which reduces source distortion [HAM 16], [BEN 16], [BOU09].

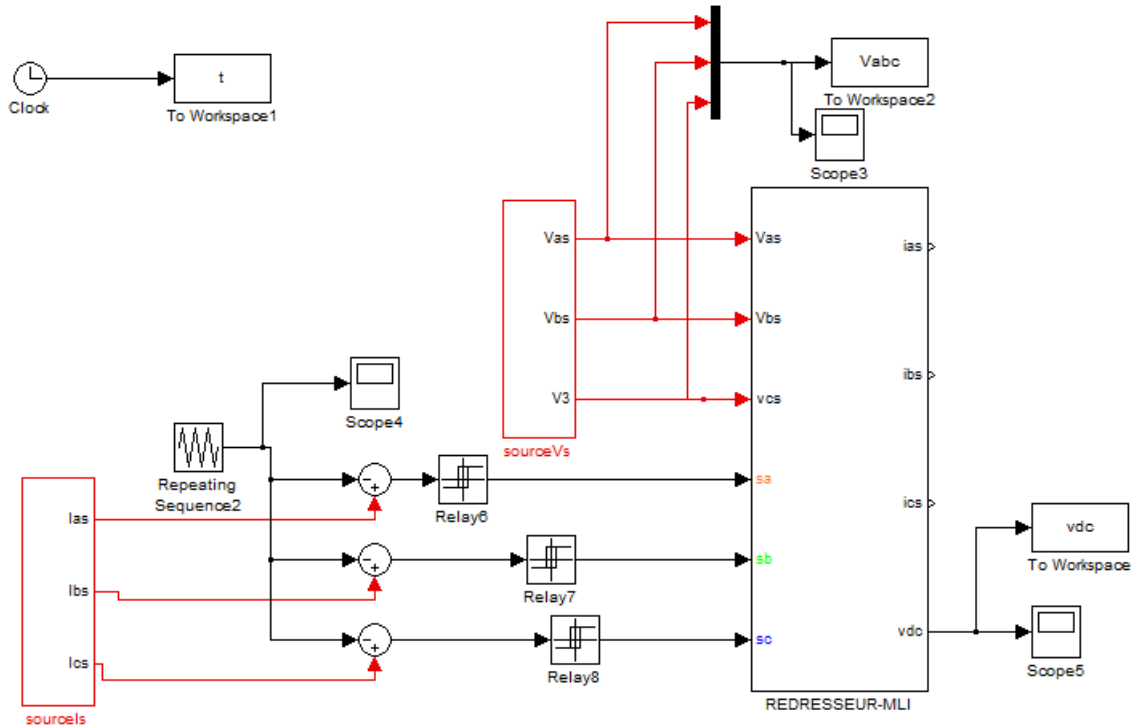


Figure.II.10. PWM Rectifier Block Diagram by MATLAB/Simulink.

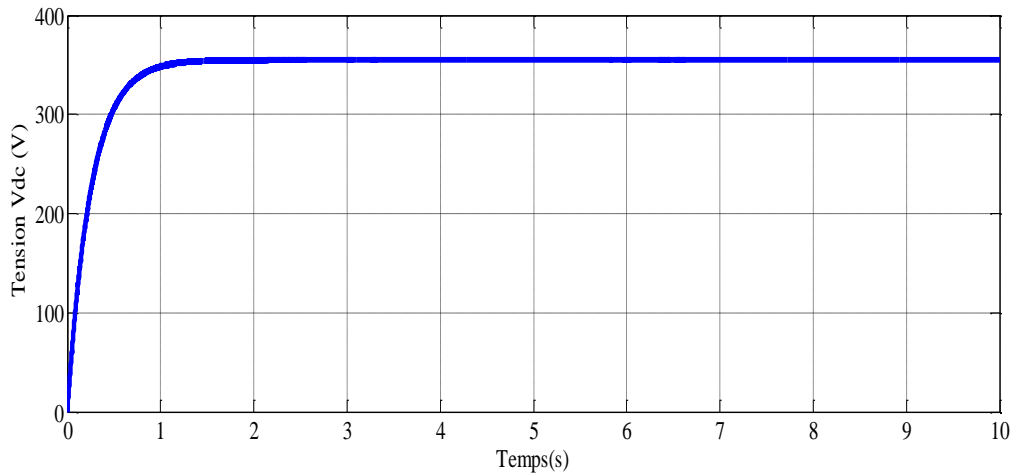


Figure.II.11. PWM Rectifier Voltage  $V_{dc}$ .

## II.8 Conclusion:

Modeling the Permanent Magnet Synchronous Machine (PMSM) is a crucial step in the development of effective and precise control systems. By using the rotating dq-reference frame, we were able to obtain a mathematical representation that simplifies the dynamic performance analysis of the machine. This model not only aids in understanding the machine's operation but also serves as a solid foundation for implementing modern control algorithms, paving the way for improved efficiency and reliability in industrial and renewable energy applications.

This chapter presents a study of all the permanent magnet synchronous generators (PMSGs), wind turbines, and PWM rectifiers used. We presented the main theories. We described the different PWM structures (no-load, on-load, and short-circuit), then we described the interaction between the wind and the wind turbine (horizontal axis type). Finally, we presented the voltage-dependent PWM rectifier modeling used for our conversion system.

In the next chapter, we will examine the predictive control used to adjust the PWM rectifier voltage.

# **Chapter III: Control of PMSM and the Proposed Hybrid Strategy**

## III.1 Introduction

Field-Oriented Control (FOC) and Model Predictive Control (MPC) are two advanced techniques widely used in electric drive systems for precise and efficient control of AC machines, particularly Permanent Magnet Synchronous Machines (PMSMs). FOC achieves dynamic decoupling of torque and flux, enabling smooth and fast responses similar to DC machines. In contrast, MPC uses a predictive model to optimize control actions in real time, considering constraints and system variations. While FOC is well-established and reliable, MPC offers greater flexibility and potential for improved performance, especially under complex operating conditions. This work investigates both approaches to enhance the control of PMSM-based systems.

This chapter investigates both control strategies and proposes a hybrid solution to improve the performance and robustness of PMSM-based system.

## III.2 Field-Oriented Control

The type of the MCC machine remains widely used due to the simplicity of its control system. This simplicity stems from the natural decoupling between the control of magnetic flux and electromagnetic torque, allowing for high dynamic performance.

Modern control techniques have sought to emulate this ease and precision of regulation offered by the DC machine. One of the most notable approaches is vector control (flux-oriented control), which is applied to alternating current machines such as the permanent magnet synchronous machine (PMSM). This technique enables the dynamic model of the machine to be decoupled similar to that of a separately excited DC machine, thereby, enhancing both steady-state and dynamic performance [Bou 14].

## III.3 Advantages and Disadvantages of Field-Oriented Control

### III.3.1 Advantages of Field-Oriented Control

- Field-Oriented control relies on the machine's dynamic (transient) model, enabling it to handle transitional operating states something that traditional control methods could not effectively achieve.
- It provides high accuracy and fast dynamic response.
- Torque control is possible even when the machine is at standstill.
- It allows for precise regulation of electrical quantities in both magnitude and phase, improving overall control quality [Ami 17].

### III.3.2 Disadvantages of Field-Oriented Control

Despite its performance advantages, rotor flux-oriented field-oriented control presents several drawbacks [Ami 17]:

- It involves relatively high implementation costs due to the need for additional components such as incremental encoders or speed estimators, as well as digital signal processors (DSPs).
- The system's sensitivity to parameter variations particularly to changes in the rotor time constant can reduce its robustness.
- A modulator is required to interface with the inverter, which can introduce delays, especially at low modulation frequencies in high-power systems. These delays may negatively affect the torque response time, posing challenges in applications like electric traction.
- The control algorithm depends on coordinate transformations that require an estimated angular position ( $\theta_s$ ), which introduces potential sources of error.
- Since the control law explicitly includes the rotational speed, sensorless systems relying on speed estimation may suffer from performance degradation due to inaccuracies in the estimated speed.

### III.4 The Principle of Field-Oriented Control for PMSM

By analyzing the system of equations, particularly the electromagnetic torque equation, it is evident that the model of the Permanent Magnet Synchronous Machine (PMSM) is nonlinear and coupled, as the torque depends on both current components  $I_d$  and  $I_q$ . The goal of Field-Oriented Control (FOC) is to transform this model into an equivalent of a separately excited DC machine, meaning a linear and decoupled model, which allows for improved dynamic performance.

Recent control strategies, such as flux-oriented control, have appear in the literature, in order to apply the stator current vector in quadrature with the rotor flux, similar to the principle in DC machines.

The simplest and most efficient approach for PMSMs is to regular  $I_d=0$ , ensuring that the stator current  $I_s$  equals  $I_q$ . This allows the torque to be controlled solely by  $I_q$ , and the speed to be regulated by the voltage component  $V_q$ , therefore, validating the operating principle of a DC motor [Deb 21].

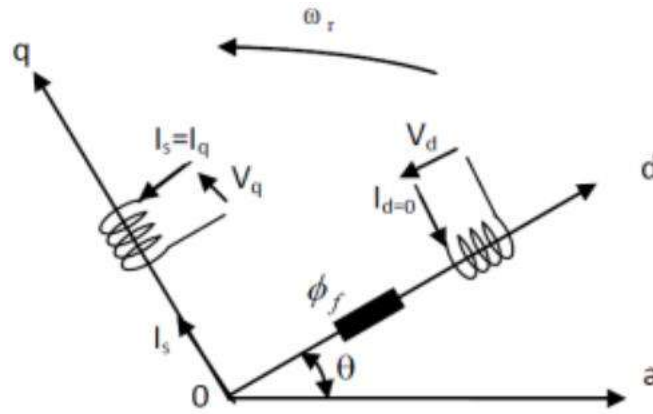


Figure III.1 .The Principle of Field-Oriented Control

### III.5 Strategy of Vector Control for PMSM

The model of the voltage-fed permanent magnet synchronous machine (PMSM) is given by the following equations:

$$\begin{cases} V_d = R_s I_d + L_d \frac{dI_d}{dt} - L_q \omega I_q \\ V_q = R_s I_q + L_q \frac{dI_q}{dt} + L_d \omega I_d + \phi_{sf} \omega \end{cases}$$

(III. 1)

$$J \frac{d\omega_r}{dx} = C_{em} - C_r - f \omega_r$$

(III. 2)

With:

$$C_{em} = (P(L_q - L_d)I_d I_q + \phi_{sf})$$

(III. 3)

Among the control strategies, one that is often used is to maintain the d-axis component at zero. This strategy allows for a simplified control law with a linear relationship between the torque and the current. This results in a characteristic that is similar to that of a separately excited DC machine.

The expression for the torque becomes:

$$C_{em} = \frac{3}{2} P \phi_f i_q$$

(III. 4)

### III.6 Decoupling by Compensation

The power supply is obtained by imposing the reference voltages at the input of the inverter control. These voltages allow to define the switching ratios on the arms of the inverter so that the voltages delivered by this inverter at the terminals of the stator of the machine are as close as possible to the reference voltages. However, it is necessary to define compensation terms, because in the stator equations, there are coupling terms between the d and q axes [Ben 05], [Mah 12].

The voltages along the (d, q) axes can be written in the following forms [Bab 01]:

$$\begin{cases} V_d = (R_s I_d + L_d \frac{dI_d}{dt}) - \omega L_q I_q \\ V_q = (R_s I_q + L_q \frac{dI_q}{dt}) + \omega (L_d I_d + \varphi_f) \\ \omega = p\omega_r \end{cases} \quad (III.5)$$

The following figure represents the coupling between the 'd' and 'q' axes:

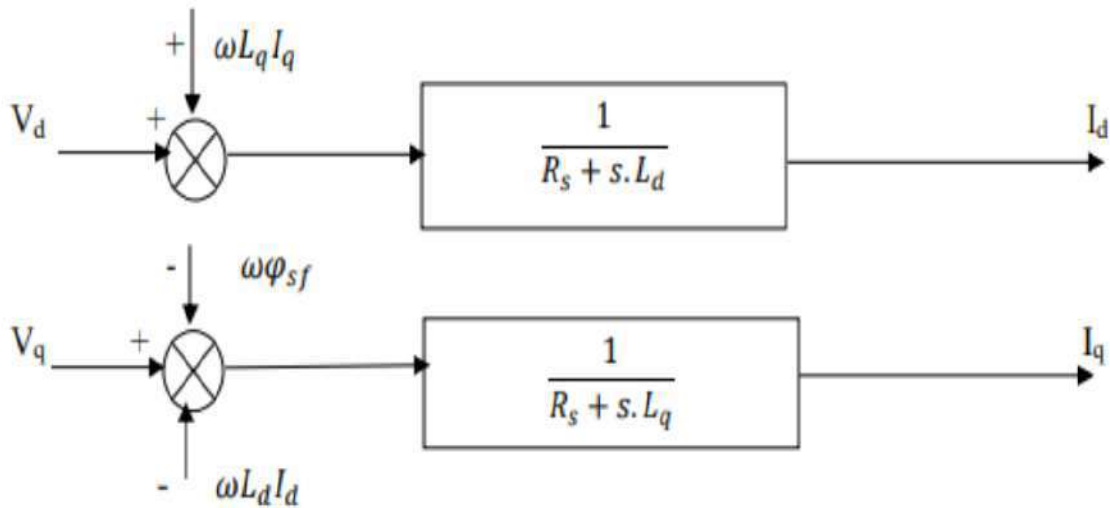


Figure III.2. General structure: (machine-decoupling by compensation).

The voltages  $v_d$  and  $v_q$  depend on both the currents on the «d» and «q» axes, so we are led to implement a decoupling. This decoupling is based on the introduction of the compensating terms  $e_d$  and  $e_q$ .

With:

$$\begin{cases} e_d = \omega L_q I_q \\ e_q = -\omega(L_d I_d + \varphi f) \end{cases}$$

(III. 6)

From equations (III.5) and (III.6), we have:

$$\begin{cases} V_d = V_{d1} - e_d \\ V_q = V_{q1} + e_q \end{cases}$$

(III. 7)

With :

$$\begin{cases} V_{d1} = (R_s + S.L_d)I_d \\ V_{q1} = (R_s + S.L_q)I_q \end{cases}$$

(III. 8)

And:

$$\begin{cases} e_d = \omega L_q I_q \\ e_q = -\omega(L_d I_d + \varphi f) \end{cases}$$

Therefore, the currents  $I_d$  and  $I_q$  are decoupled. The current  $I_d$  depends only on  $V_{d1}$ , and  $I_q$  depends only on  $V_{q1}$ . From equation (III.6), the currents  $I_d$  and  $I_q$  are written as follows:

$$\begin{cases} I_d = \frac{V_{d1}}{(R_s + S.L_d)} \\ I_q = \frac{V_{q1}}{(R_s + S.L_q)} \end{cases} \quad (III.9)$$

S: Laplace Operator.

The regulation principle involves regulating the stator currents based on the desired reference values using conventional controllers. The block diagram illustrating the regulation of stator currents is represented in the figure below:

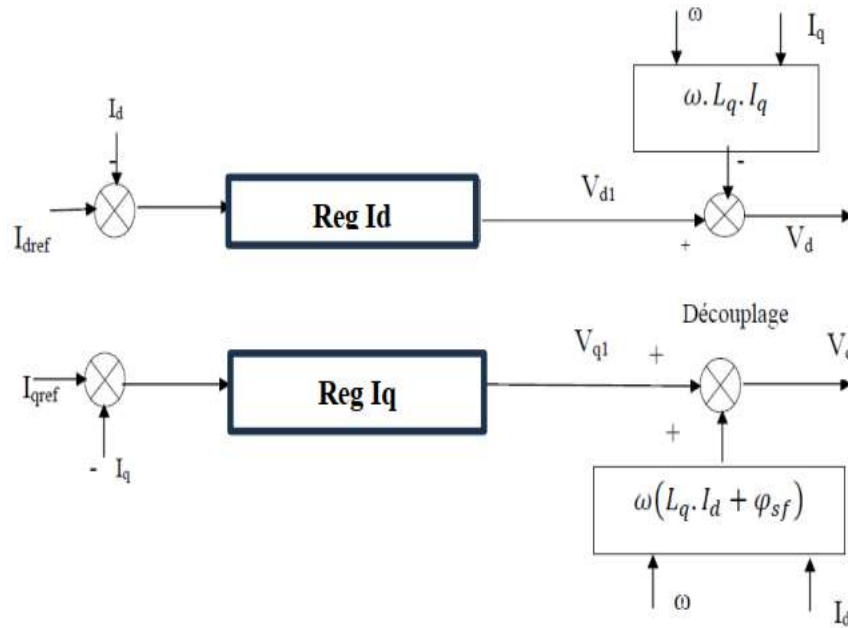


Figure III.3. Description of the couplings.

With:

$V_{d1}$ : The voltage at the output of the 'Id' current regulator

$V_{q1}$ : The voltage at the output of the 'Iq' current regulator

If we combine the machine with the compensation block, we obtain figure III.4.

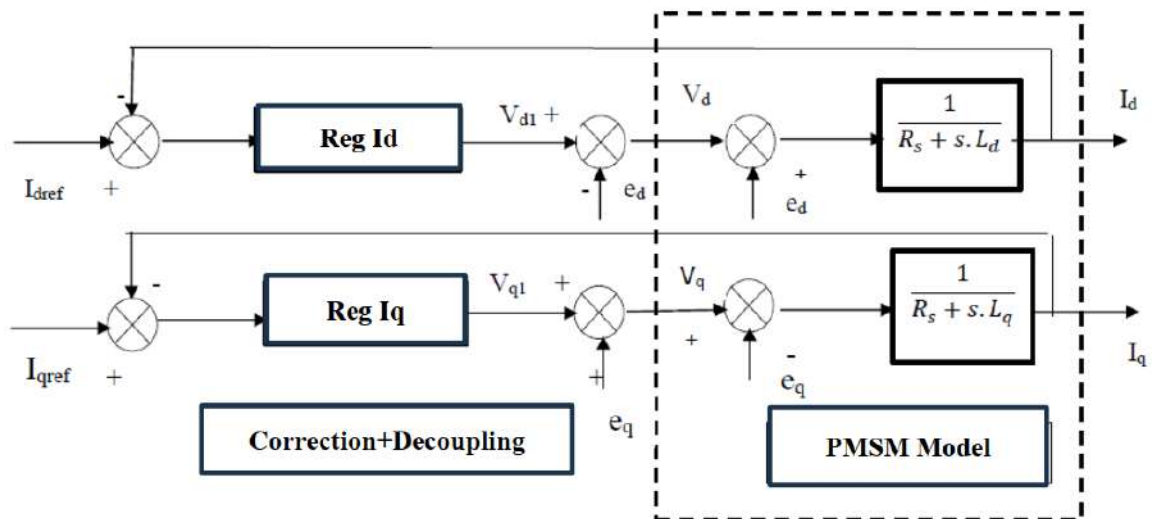


Figure III.4 Principle of decoupling by compensation.

## III.7 Field-Oriented Control of PMSM

### III.7.1 Global Diagram of the Field-Oriented Control for the (PMSM)

In the  $d$  and  $q$  axes, field-oriented control is commonly used for voltage-supplied and current-regulated machines. This design enhances the torque control dynamics while avoiding the drawbacks of current supply. Figure (III.5) shows the block diagram for speed regulation of the Voltage-Supplied Permanent Magnet Synchronous Machine (PMSM) controlled by field orientation.

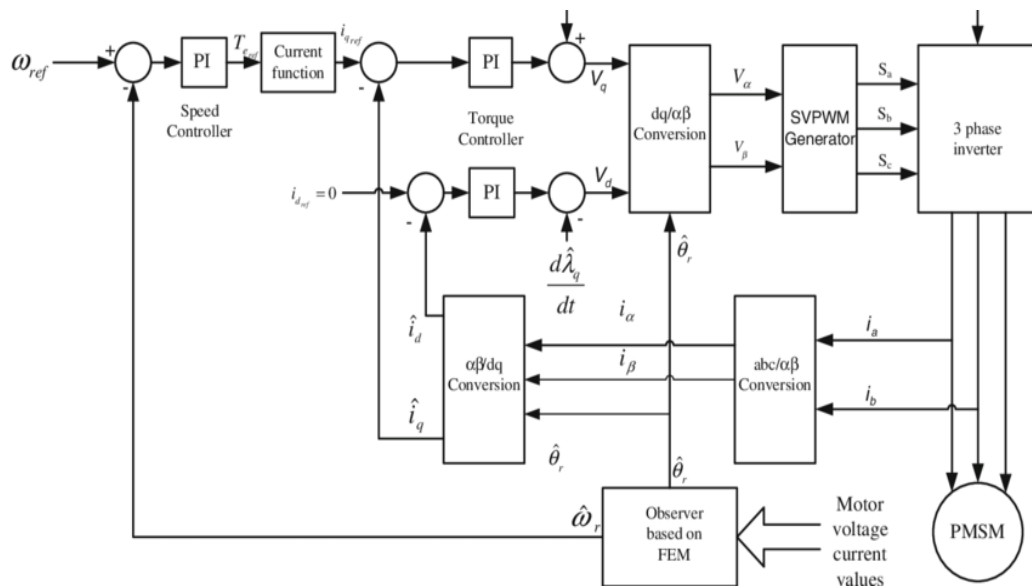


Figure III.5 Global Diagram of the Field-Oriented Control for the (PMSM).

The main components of field-oriented control are the speed regulation loop, the current regulation loops for  $I_d$  and  $I_q$ , and the Park and Concordia transformations [Djo 15]. The speed is regulated through the outer loop of the system, where the output of its controller is the reference electromagnetic torque  $C_{emref}$  or the reference current  $I_{qref}$ . This reference current is limited to take into account the inverter characteristics and the machine's overload.

The reference current  $I_{qref}$  is compared to the actual measured value  $I_q$ . The error generated by this comparison drives the input of the reference voltage controller  $V_{dref}$ . In parallel with this inner loop, there is a regulation loop for  $I_d$ . The reference current  $I_d$  is kept at zero. The outputs of the  $I_d$  and  $I_q$  controllers provide the reference voltages  $V_{dref}$  and  $V_{qref}$ , and through the Park transformation, the reference voltages  $V_{as}$ ,  $V_{bs}$ , and  $V_{cs}$  are obtained, which are the voltages used for controlling the inverter with PWM control [Djo 15].

### III.7.2 Regulator design

The role of the regulators is to maintain the output variable equal to the reference value, despite the presence of internal or external disturbances [Ami 07].

Once decoupling between the d and q axes is achieved, control is carried out using Proportional-Integral (PI) regulators. The **integral action** serves to minimize the error between the reference and the controlled variable, while the **proportional action** governs the system's dynamic response speed [Ben 05].

The PI regulator combines proportional and integral actions in parallel, as illustrated in Figure (III.6). The relationship between the output  $Ur(t)$  and the error signal  $\varepsilon(t)$  is expressed by the following equation:

$$Ur(t) = kp\varepsilon(t) + ki \int_0^t \varepsilon(t)dt \quad (III.10)$$

The transfer function is given by:

$$\frac{Ur}{\varepsilon} = kp + \frac{ki}{s} \quad (III.11)$$

Where:

- $kp$  : Proportional gain, which determines the immediate response of the system to the error signal.
- $ki$ : Integral gain, which eliminates the steady-state error by integrating the error over time.

The regulator can also be expressed in the following form:

$$P.I \rightarrow \frac{Ur}{\varepsilon} = \frac{1+sT1}{sT2}$$

(III. 12)

Where:

$$\begin{cases} k_p = \frac{T_1}{T_2} \\ k_i = \frac{1}{T_2} \end{cases}$$

(III. 13)

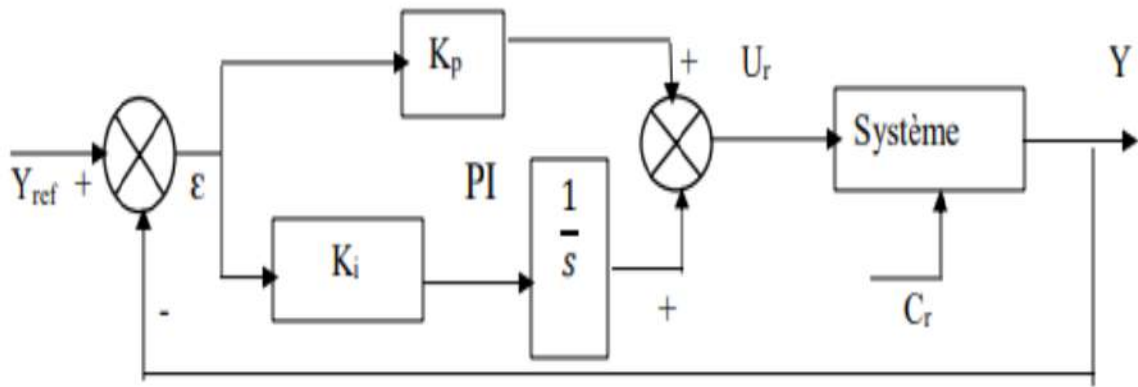


Figure III.6 .PI Regulator design.

### III.7.2.1 Regulator Tuning

Since the machine is decoupled along the two axes  $d$  and  $q$ , control on the  $d$ -axis is performed using a single control loop, which regulates the current along this axis. In contrast, the  $q$ -axis employs a cascaded dual-loop structure:

- Inner loop: Responsible for regulating the  $q$ -axis current.
- Outer loop: Dedicated to speed control.

This architecture allows for the separation of current and speed dynamics, enabling more precise and stable control [Ala 02].

#### III.7.2.1.1 $I_q$ Current Regulator

The control of the Permanent Magnet Synchronous Machine (PMSM) is achieved by regulating the currents  $I_d$  and  $I_q$ . The system includes a speed control loop, which generates the reference signal  $I_{qref}$ , while the  $I_d$  current is maintained at zero ( $I_d=0$ ). Proportional-Integral (PI) regulators are employed to ensure zero steady-state error ( $\epsilon=0$ ), thus enabling accurate tracking of the reference currents [Aid 13],[Ade 07],[Bel 01].

Given that:

$$I_q = \frac{V_{q1}}{R_S + sL_q}$$

(III. 14)

Given that the general form of the PI regulator is expressed as:

$$\frac{1+sT1}{sT2}$$

This leads to the block diagram shown in Figure (III.7), which illustrates the control structure for the  $q$ -axis current using a PI regulator.

This representation integrates the proportional and integral effects in a standard form, where:

- $T1$ : Time constant associated with the proportional action.
- $T2$ : Time constant associated with the integral action.

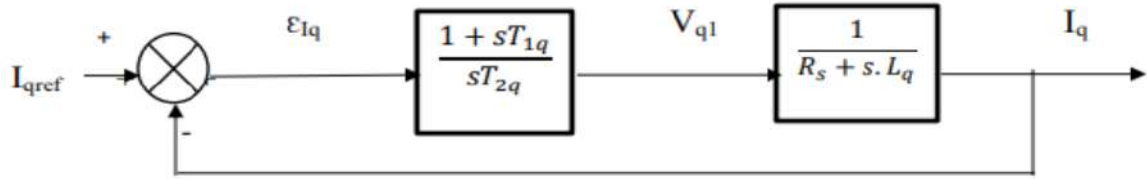


Figure III.7.  $I_q$  Current Control Loop

The **Open-Loop Transfer Function (OLTF)** for the system shown in Figure (III.7) is:

$$OLTF = \frac{1 + sT_{1q}}{sT_{2q}(R_s + sL_q)}$$

(III. 15)

$$OLTF = \frac{1 + sT_{1q}}{sT_{2q}R_s \left(1 + s\frac{L_q}{R_s}\right)}$$

(III. 16)

By using the pole compensation method, we obtain:

$1 + sT_{1q} = 1 + s\frac{L_q}{R_s}$  This translates to the following condition:

$$\frac{L_q}{R_s} = T_{1q} = \tau_q$$

(III. 17)

$\frac{L_q}{R_s}$ :Electrical Time Constant

If we replace the constant with its value, equation (III.15) into equation (III.17), we get:

$$OLTF = \frac{1}{sR_sT_{2q}}$$

(III. 18)

For the Closed-Loop Transfer Function (CLTF):

$$CLTF = \frac{OLTF}{1 + OLTF}$$

(III. 19)

$$CLTF = \frac{1}{1 + sR_sT_{2q}} \text{ Of the form:}$$

$$\frac{1}{1 + s\tau_q}$$

(III. 20)

By identification, we find:

$$\tau q = R_s T_{2q} \rightarrow T_{2q} = \frac{\tau q}{R_s}$$

(III. 21)

By imposing the reference time:

$$T_r = 3 \tau q \text{ (Criterion of } \pm 5\%)$$

(III. 22)

We have:

$$T_{2q} = \frac{T_r}{3R_s}$$

(III. 23)

$T_r$ : Imposed response time.

If we substitute equation (III.23) into (III.13), we finally obtain:

$$\begin{cases} k_p = \frac{3L_d}{T_r} \\ k_i = \frac{3R_s}{T_r} \end{cases}$$

(III. 24)

### III.7.2.1.2 $I_d$ Current Regulator

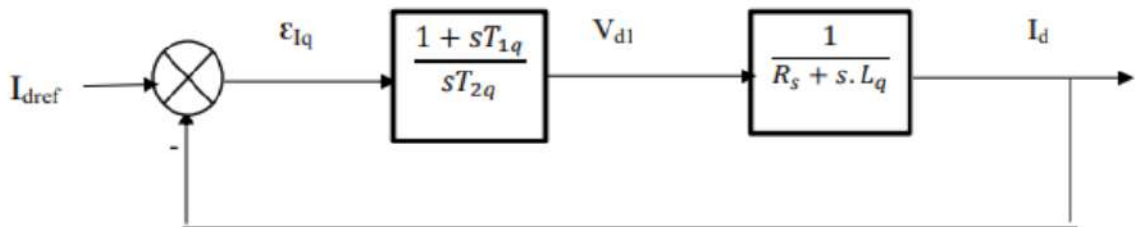


Figure III.8. Current regulation loop of  $I_d$ .

In the same way as the calculation of the  $I_q$  current regulator, the  $I_d$  current regulator is determined with [Sek 08],[Att 11]:

$$\frac{L_d}{R_s} = T_{d1} = \tau d$$

(III.25)

On Imposing

$$T_r = 3\tau d = \frac{3R_s}{k_{id}} \quad (III.26)$$

$$\begin{cases} k_{id} = \frac{3R_s}{T_r} \\ k_{pd} = \frac{3L_d}{T_r} \end{cases} \quad (III.27)$$

### III.8 History of Predictive Control

Predictive control is a relatively recent technique, which has only really taken off since the 1980s, thanks to the work of DW Clarke and his team at Oxford. However, this control technique, which can be linked to the family of model predictive controls (MPC), has attracted interest in the industrial field since the end of the 1970s. In 1978, J. Richalet published the first results obtained in industrial applications and in 1979, Shell engineers CR Cutler and DM Prett shared their experience on a catalytic cracker. In 1985, DW Clarke presented the first version of the generalized predictive control (GPC). It was not until 1987 that the first results obtained by J. Richalet on fast electromechanical systems, such as robot axis controls, were published [Mig 04] [Alb 04].

Predictive control has gained popularity in the chemical and petroleum industries, partly because this technique provides a methodology that can systematically take constraints into account when designing and implementing the control law.

### III.9 Principle of Predictive Control

Predictive control, also called compensation or anticipatory correction, is an advanced control technique. Its objective is the control of complex industrial systems with multiple inputs and outputs where the simple PI regulator is insufficient. The principle of this control is to use a dynamic model of the controlled process inside the controller in real time in order to anticipate the future behavior of the process. Predictive control is one of the internal model control techniques. It is particularly interesting when the systems have significant delays or inverse responses and are subject to numerous disturbances. This control technique was invented by J.RICHALET in 1978 and generalized by DW Clarke in 1987 in collaboration with large industrial groups [Mer 07] [Ais 07].

In its fundamentals, predictive control defines at each instant the best control to apply to the process, considering the desired reference, the current state of the system and a prediction of the near future obtained using a behavioral model. This predictive characteristic, which can also be extended to known disturbances, gives the controlled system a strong dynamic potential.

Generally speaking, the internal model predictive control algorithm performs the same steps at each sampling instant, as shown in Figure III.11.

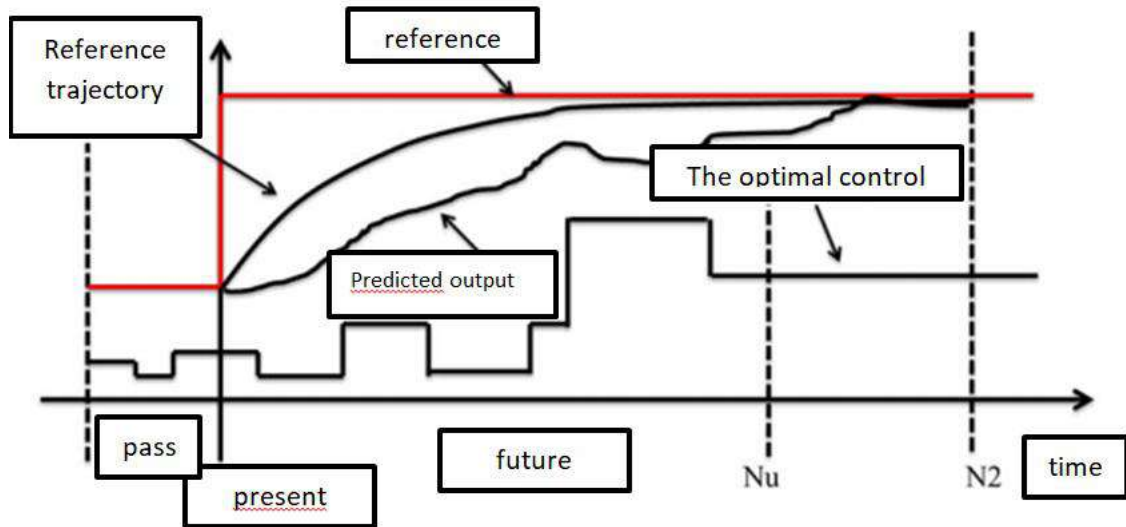


Figure III.9. Principle of Predictive Control.

Calculation of predictions of controlled variables up to a time horizon  $N_2$  using the internal model of the process.

- Development of a reference trajectory to follow.
- Calculation of a sequence of future samples of optimal orders minimizing a cost function over time horizon  $N_u$ .
- Only the first element of the calculated control sequence is applied to the system during the next sampling. All these steps will then be repeated, this is the vanishing horizon principle [Mer 07] [Ais 07].

However, with the incredible advances in semiconductor and microprocessor technologies, interest in MPC applications has significantly increased over the past few decades. MPC includes a large family of controllers, and the common feature among all these controllers is the use of a model of the system to predict the future behavior of the controlled variables over a predefined prediction horizon and to select the optimal control action by minimizing a cost function.

The discrete model used for prediction can be expressed as a state-space model:

$$\begin{cases} x(k+1) = Ax(k) + Bu(k) \\ y(k) = Cx(k) + Du(k) \end{cases}$$

(III. 28)

- The cost function, which represents the desired behavior of the controlled system, is defined by considering the reference variables, the future states of the controlled variables, and their future optimal values. Generally, for a prediction horizon of  $N$  steps, the cost function is written as:

$$F = f(X(k), u(k), \dots, u(k + N)) \quad (\text{III. 29})$$

Minimizing this function allows the selection of the optimal control action that should be applied by the predictive controller. Thus, the controller applies only the first optimal control input where the cost function is minimized over the sampling period. The operating principle of MPC is summarized in Figure III.11.

The future values of the system's states are predicted up to a predefined time horizon  $k + N$  using the system model and the available information (measurements) up to the current time  $k$ . The optimal control sequence is obtained by minimizing the cost function, and the first element of this sequence is applied. This process is repeated at each sampling step by taking into account the newly measured data [Bou 22].

### III.10 Advantages of Model Predictive Control (MPC)

Model predictive control has several advantages:

- The concept is very intuitive, easy to understand and implement.
- It can be applied to a wide variety of systems.
- Multivariable systems as well as external constraints can be considered.
- Nonlinearities can be easily integrated into the model.
- This method is suitable for incorporating modifications and extensions depending on specific applications.

### III.11 Model formulation

All predictive control algorithms differ from each other only in the model used to represent the process and in the cost function to be minimized. The process model can take different representations (by transfer function, by state variables, impulse response, etc.). For our formulation, the structure adopted here is the CARMA form [Cam 03] [Mal 00]:

$$y(t) + a_1 y(t - 1) + \dots + a_{na} y(t - na) = b_0 u(t - d) + b_1 u(t - d - 1) + \dots + b_{nb} u(t - d - nb) + e(t)$$

(III.30)

With :

$y(t)$ : process output

$u(t)$ : command applied to the input

$d$ : system delay, (electric machines are considered to be fast processes, we most often take  $d = 1$ ).

$q - d$ : delay operator ( $z^{-d}y(t) = y(t - d)$ ).

$e(t)$ : term linked to the disturbance.

The polynomials  $A(z^{-1})$  and  $B(z^{-1})$  are defined as follows:

$$\begin{aligned} A(z^{-1}) &= 1 + a_1z^{-1} + \dots + a_{na}z^{-na} = 1 + \sum_{i=1}^{na} a_i z^{-i} \\ B(z^{-1}) &= b_0 + b_1z^{-1} + \dots + b_{nb}z^{-nb} = \sum_{i=0}^{nb} b_i z^{-i} \end{aligned} \quad (III.31)$$

The digital representation model for the GPC is illustrated by the following Figure III.13:

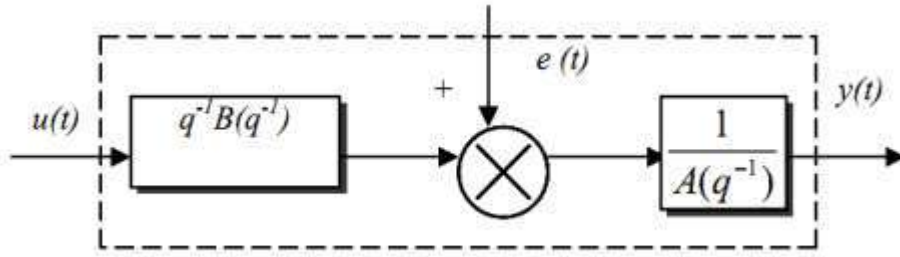


Figure III.10 .Digital representation model for the GPC.

The form of the term related to the disturbance defines the modeling system (process + disturbance):

$$e(t) = C(z^{-1}) \frac{\xi(t)}{D(z^{-1})} \quad (III.32)$$

$\xi(t)$  : is a centered white noise (its average value is zero).

$$C(z^{-1}) = 1 + c_1z^{-1} + \dots + c_{nc}z^{-nc} \quad (III.33)$$

In the CARMA model, we reason on an incremental model of the system, therefore the polynomial  $D(z^{-1})$  is taken as being the difference operator  $\Delta(z^{-1})=1-z^{-1}$  (integrator). The goal sought with the introduction of an integrator is the cancellation of any static error with respect to a setpoint or a constant disturbance. We will subsequently take  $C(z^{-1})=1$ . Finally, the CARMA model from which the expression of the GPC control law will be derived is given by the following relation [Bar 08], [Mez 09]:

$$A(z^{-1})y(t) = z^{-1}B(z^{-1})u(t) + \frac{\xi(t)}{\Delta(z^{-1})} \quad (III.34)$$

### III.12 Predictor development

For simplicity during development  $C(z^{-1})$  is chosen to be equal to 1, we obtain the model [Cam 03]:

$$\left[ A(z^{-1})y(t) = B(z^{-1})z^{-d}u(t-1) + \frac{e(t)}{\Delta} \right] \times \Delta E(z^{-1})z^j \quad (\text{III.35})$$

To derive the  $j$ -step forward predictor, we consider the identity

$$1 = E_j(z^{-1})A(z^{-1}) + z^{-j}F(z^{-1}) \quad (\text{III.36})$$

With

$$A(z^{-1}) = \Delta A(z^{-1}) \quad (\text{III.37})$$

$E_j(z^{-1})$ : is a polynomial of order  $(j-1)$

$F(z^{-1})$ : is a polynomial of order  $(na)$

Multiplying equation (III.8) by the term  $\Delta E(z^{-1})z^j$  we obtain:

$$A(z^{-1})E_j(z^{-1})y(t+j) = E_j(z^{-1})B(z^{-1})\Delta u(t+j-d-1) + E_j(z^{-1})e(t+j) \quad (\text{III.38})$$

Using the Diophantine identity (III.7) we obtain:

$$\left( 1 - z^{-j}F_j(z^{-1}) \right) y(t+j) = E_j(z^{-1})B(z^{-1})\Delta u(t+j-d-1) + E_j(z^{-1})e(t+j) \quad (\text{III.39})$$

We therefore deduce the output equation  $y(t+1)$

$$y(t+j) = F_j(z^{-1})y(t) + E_j(z^{-1})B(z^{-1})\Delta u(t+j-d-1) + E_j(z^{-1})e(t+j) \quad (\text{III.40})$$

Since  $E_j(z^{-1})$  is of degree  $(j-1)$  the product  $E_j(z^{-1})$  is zero, which proves the robustness of the algorithm whose noise components are all zero in the future, which makes this type of predictor optimal and robust, hence the predictor model is as follows:

$$\check{y}\left(t + \frac{j}{t}\right) = G_j(z^{-1})\Delta u(t+j-d-1) + f_j(t+j) \quad (\text{III.41})$$

With :

$$\Delta u(t+j-d-1) = u(t+j-d-1) - u(t+j-d-2) \quad \text{For} \quad 1 \leq j \leq N_u$$

$$G_j(z^{-1}) = E_j(z^{-1})B(z^{-1})$$

$$f_j(t+j) = F_j(z^{-1})y(t) \quad \text{For} \quad j = 1 \dots N_2$$

$$F_j(z^{-1}) = f_{j,0} + f_{j,1}z^{-1} + \dots + f_{j,na}z^{-na}$$

$$E_j(z^{-1}) = e_{j,0} + e_{j,0}z^{-1} + \dots + e_{j,(j-1)}z^{-(j-1)}$$

So long-term prediction is done by the recursive calculation of the polynomial  $G_j(z^{-1})$  and the function  $f_j(t+j)$

To calculate  $G_{j+1}(z^{-1}) = E(z^{-1})_{j+1}B(z^{-1})$  et  $f_{j+1}(t+j) = F_{j+1}(z^{-1})y(t)$  we proceed from the recursion of the Diophantine equation used previously.

### III.13 Optimization criterion

Once the predictions have been made, we must find the future control sequence to apply to the system to reach the desired set point by following the reference trajectory. To do this, we minimize a cost function that differs depending on the methods, but generally this function contains the quadratic errors between the reference trajectory and the predictions over the prediction horizon as well as the variation of the control. This cost function is as follows [Pat 96]:

$$J_{GPC} = \sum_{j=N_1}^{N_2} [w(t+j) - \hat{y}(t+j)]^2 + \lambda \sum_{j=1}^{N_y} \Delta u(t+j-1)^2 \quad (\text{III.42})$$

With:

$w(t+j)$ : Instruction applied at the moment  $(t+j)$ ;

$\hat{y}(t+j)$ : Predicted output at the moment  $(t+j)$ ;

$\Delta u(t+j-1)$ : Command increment at the moment  $(t+j-1)$ ;

$N_1$ : Minimum prediction horizon on the output;

$N_2$ : Horizon of maximum prediction on the output with  $\geq N_2 N_1$ ;

$N_u$ : Prediction horizon on the order;

$\lambda$ : Weighting coefficient on the order.

The following assumption is made on the order:  $\Delta u(k+j) = 0$  for  $j \geq N_u$ .

Analytical minimization of this function provides the sequence of future commands, of which only the first will actually be applied to the system. The procedure is iterated again at the next sampling period according to the rolling horizon principle.

The expression of the criterion calls for several remarks

- If we actually have the setpoint values in the future, we use all this information between the horizons  $N_2$  and  $N_1$  in such a way as to make the predicted output converge towards this setpoint.
- The incremental aspect of the system is found by considering  $\Delta u$  in the criterion
- The coefficient  $\lambda$  makes it possible to give more or less weight to the command in relation to the output, so as to ensure convergence when the starting system presents a risk of instability [Nic 06].

### III.14 Design of Model Predictive Control for PMSM

In the design phase of MPC for the control of power converters, the following steps are essential:

- Modeling the power converter and identifying all possible switching states and their relationship with the input or output voltages or currents.
- Defining a cost function that represents the desired behavior of the system.
- Developing the discrete model that enables the prediction of the future behavior of the variables to be controlled.

To obtain a discrete-time model, it is necessary to use discretization methods. To approximate derivatives, Euler's method is used, where the derivative of a variable  $x$  can be expressed as:

$$\frac{dx}{dt} = \frac{(x(k+1)-x(k))}{T_s}$$

(III.51)

where  $T_s$  is the sampling period.

A general diagram of MPC dedicated to the control of power systems and electric drives is presented in Figure .14.

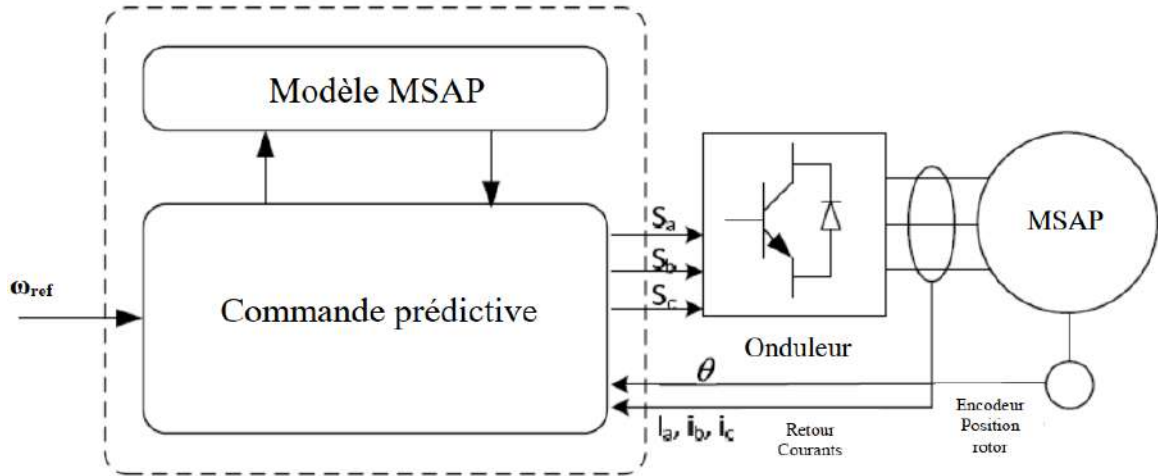


Figure III.11. Principle diagram of predictive control.

The power converter can have any topology and any number of phases, while the load represented in Figure 2.2 can be an electric machine, a grid, or any other active or passive load. In this diagram, the measured variables  $x(k)$  are used in the model to calculate the predictions  $x(k+l)$  of the controlled variables for each possible iteration; that is, the switching state, voltages, and currents. These predictions are evaluated using a cost function that takes into account the reference values  $x_{ref}(k)$  as well as the constraints imposed by the type of control applied. Thus, the optimal switching state SSS is selected and applied to the power converter [Bou 22].

### III.15 Structure of the Predictive Control Algorithm for the Inverter

The principle of predictive control can be summarized by the following steps [Bou 22]:

- Measure the variables at instant  $k$ .
- Use the previous measurements to calculate their prediction at instant  $(k+1)$ .
- Formulate a cost function to minimize, based on the desired control quantities.
- For each sampling period, evaluate the cost function for the different voltage vectors of the inverter.
- The optimal switching state  $S_{opt}$  that minimizes the cost function will be selected, so that the corresponding voltage vector  $V_{opt}$  can be applied to the three phases of the motor during the next sampling period.

All the above steps are repeated at each sampling period for the updated references and measurements.

### III.16 Model FOC and MPC of the PMSGs by MATLAB/Simulink

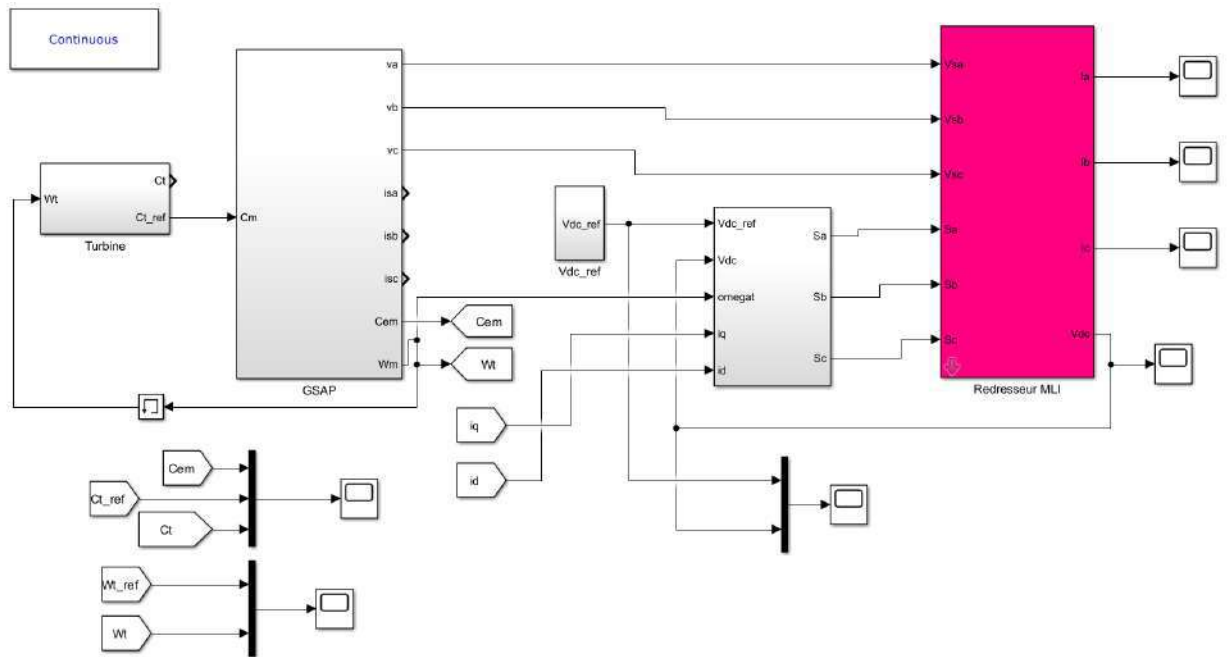


Figure III.12. Model FOC of the PMSGs by MATLAB/Simulink.

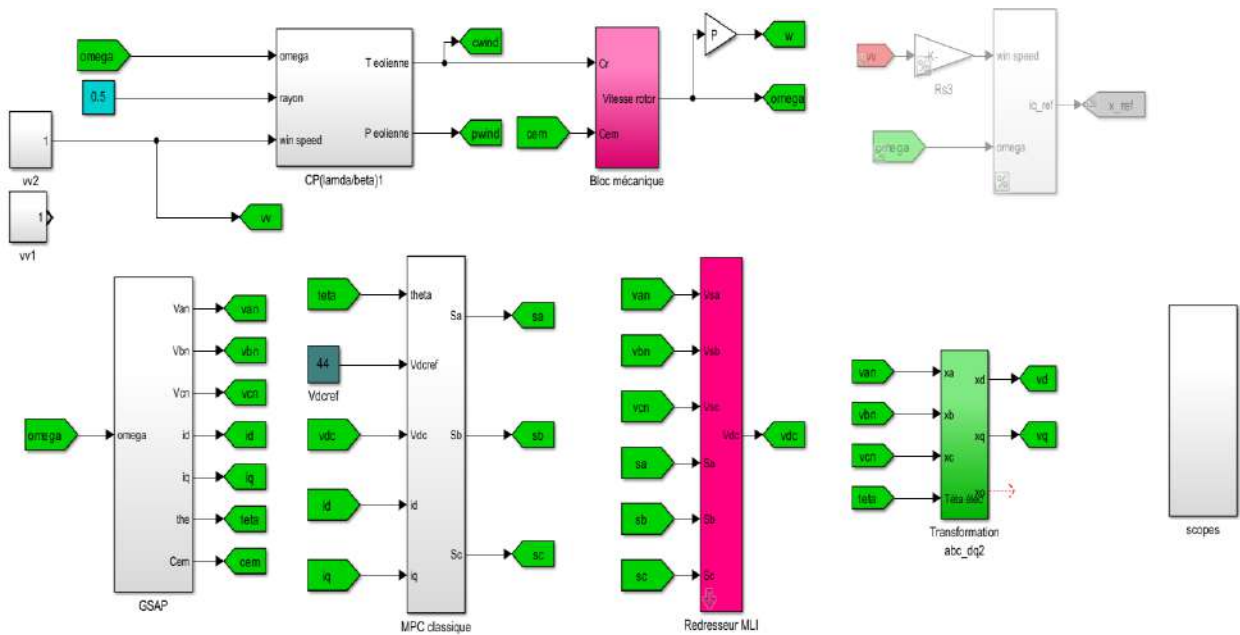


Figure III.13. Model MPC of the PMSGs by MATLAB/Simulink.

### III.17 Simulation results

In this section, we will present the simulation results to validate the predictive control applied to the PMSM, considering a 1.5 kW wind turbine whose parameters are given in (Appendix A). The predictive control strategy is implemented at the voltage rectifier level of the GSAP,

under load conditions, where the reference voltage amplitude is initially set to a constant value, and the rectifier input voltage is set to 350 V.

The results obtained are illustrated in Figures III.18 and III.25, respectively, showing :

**Figures III.18 & III.19:** These show the *three-phase stator voltages ( $V_{abc}$ )* under two control scenarios. The zoomed view in Figure III.19 reveals that predictive control significantly reduces voltage oscillations and ensures faster stabilization, indicating better dynamic performance and voltage regulation. the phase current and its harmonic spectrum, with adjustment based on the proposed technique.

**Figures III.20 & III.21:** These present the *stator currents ( $I_{abc}$ )*. Under predictive control, the current waveforms are smoother with fewer distortions, confirming an improvement in current quality and reduced harmonic content.

**Figures III.22 to III.23:** These illustrate the *DC bus voltage and rectified voltage behavior* in different test cases. Predictive control ensures quicker convergence to the reference value (typically 350 V) and better voltage stability, demonstrating its effectiveness in minimizing steady-state errors and handling dynamic load changes.

**Figure III.25:** This shows the *mechanical speed of the generator*. The speed response under predictive control is smooth and stable, reaching steady-state quickly, which highlights the system's robustness and efficient electromechanical coupling.

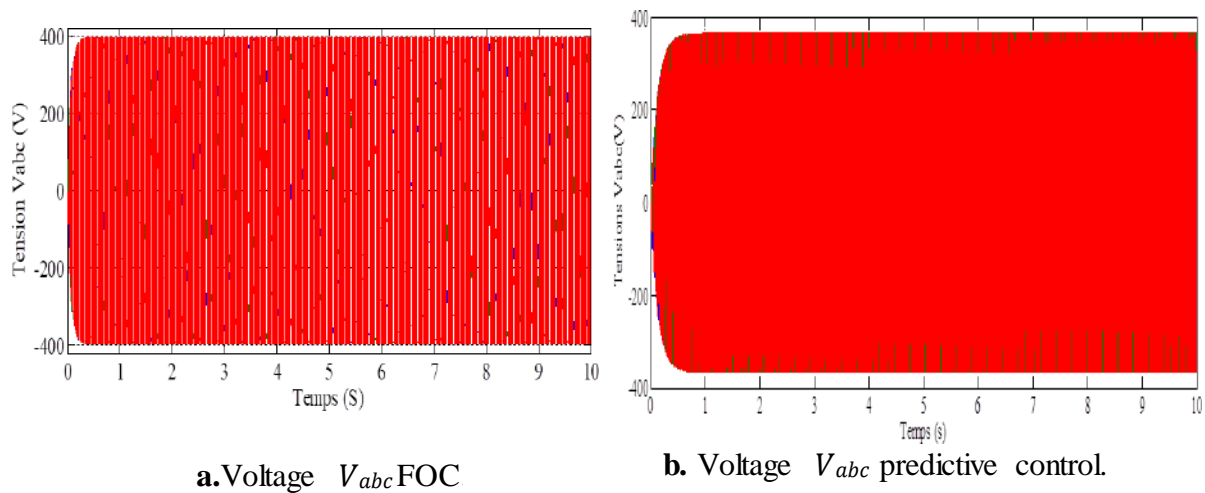
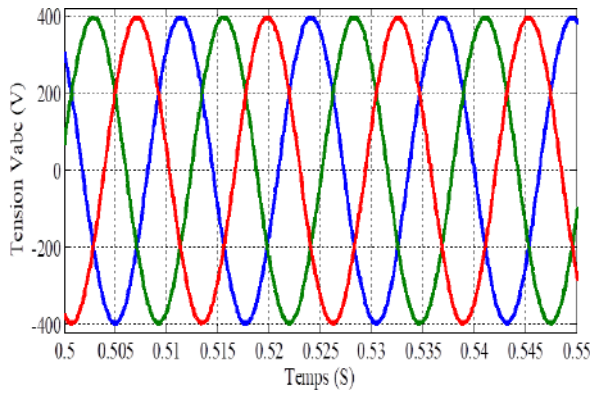
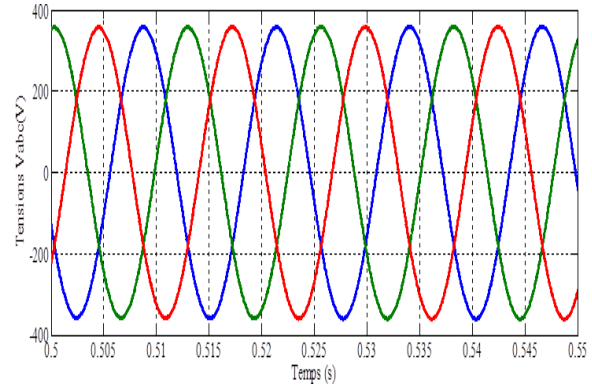


**Figure. III.14. Voltages  $V_{abc}$  in two simulation cases.**

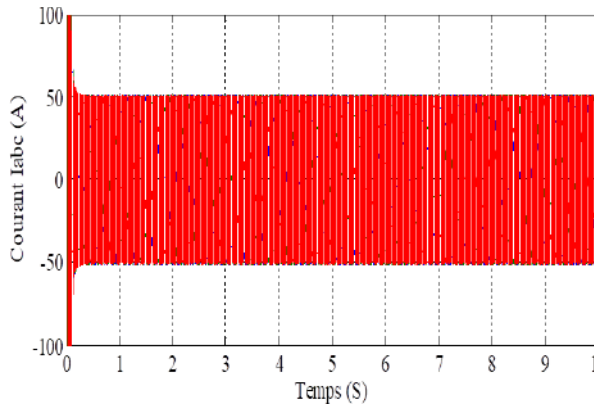


a. Voltages  $V_{abc}$  FOC.

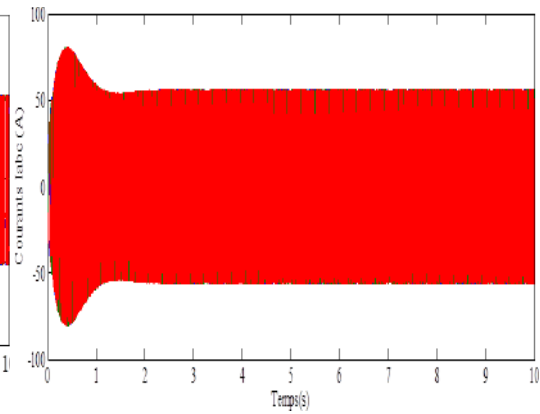


b. Voltage  $V_{abc}$  predictive control.

Figure. III.15. Voltages  $V_{abc}$  in two simulation cases with zoom.

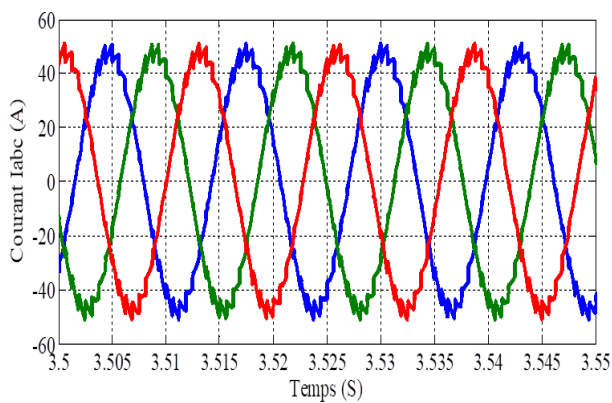


a. Current  $I_{abc}$  FOC.

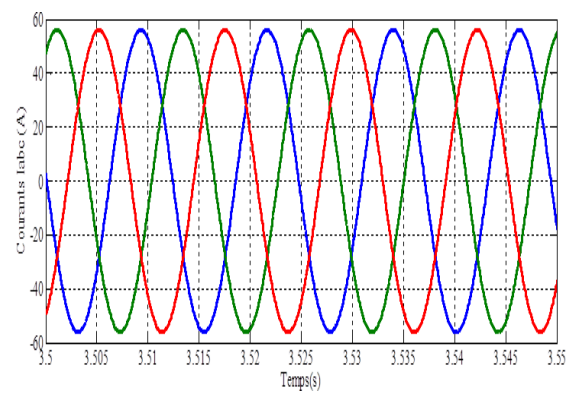


b. Current  $I_{abc}$  predictive control.

Figure. III.16. Current  $I_{abc}$  in two simulation cases.

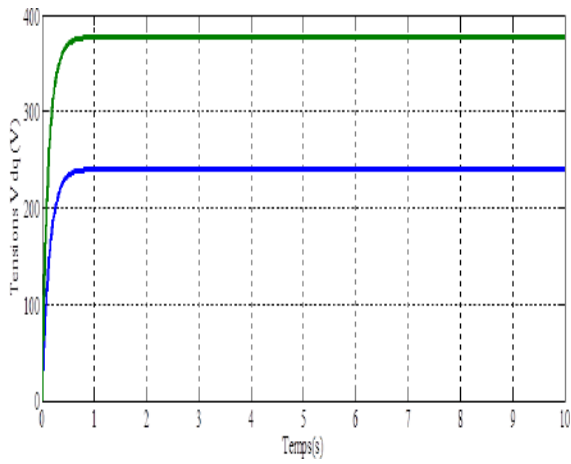


a. Current  $I_{abc}$  FOC.

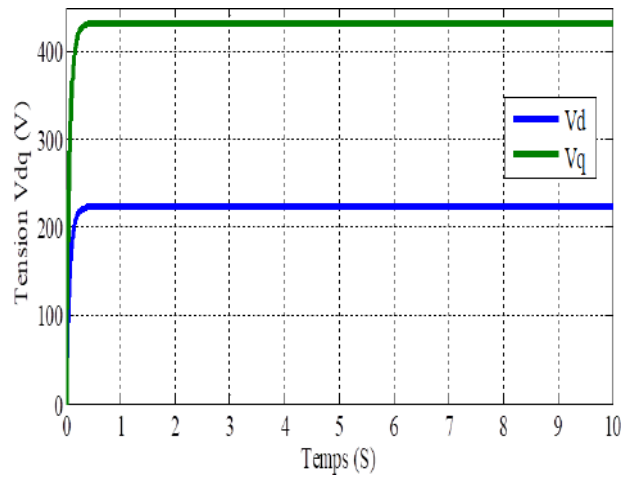


b. Current  $I_{abc}$  predictive control.

Figure. III.17. Current  $I_{abc}$  in two simulation cases with zoom.

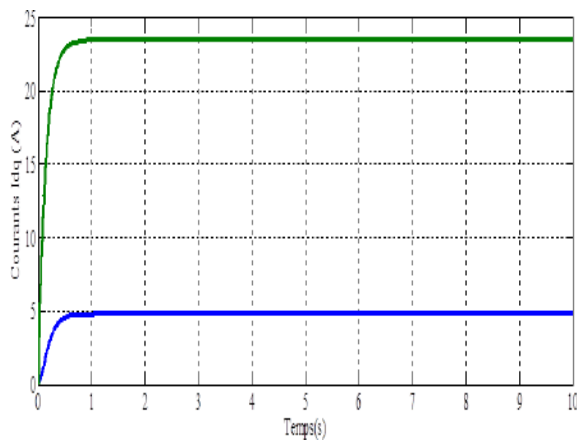


a. Voltage  $V_{dq}$  FOC.

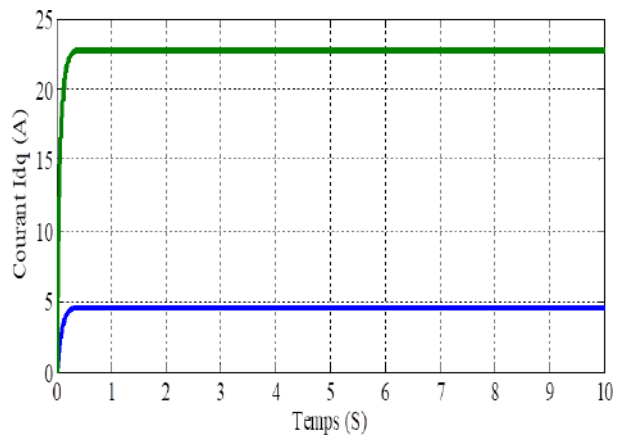


b. Voltage  $V_{dq}$  predictive control.

Figure. III.18. Voltage  $V_{dq}$   $I_{abc}$  in two simulation cases.

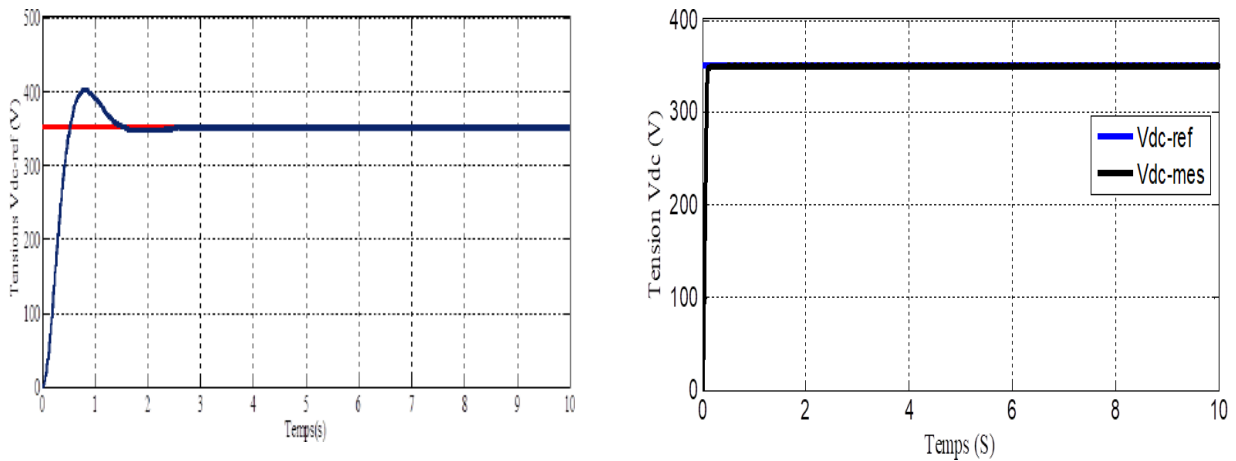


a. Current  $I_{dq}$  FOC.



b. Current  $I_{dq}$  predictive control.

Figure. III.19. Current  $I_{dq}$  in two simulation cases.



a. PWM rectifier voltage  $V_{dc}$ .

b. Predictive control voltage  $V_{dc}$ .

Figure. III.20. Voltage  $V_{dc}$  in two simulation cases.

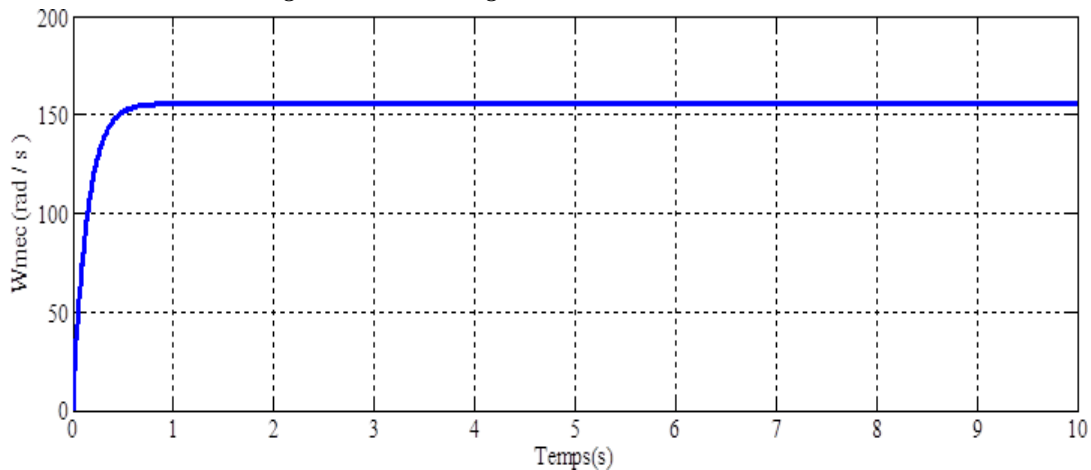


Figure. III.21. Mechanical speed.

### III.18 Conclusion

Both Field-Oriented Control (FOC) and Model Predictive Control (MPC) offer effective solutions for high-performance control of electric machines, particularly PMSMs.

The theoretical study of model predictive control (MPC) based on the possible switching states generated by a static converter (rectifier) and its application to the permanent magnet synchronous based on the comparison between and to improve the dynamic performance of the PMSM presented in this chapter. Also we have presented application of the Field-Oriented Control (FOC) at the level Permanent Magnet Synchronous Machines (PMSM).

Firstly, the PMSM was powered by a PWM rectifier. Second, the predictive control technique was implemented in the PMSM model, after which the simulation results in MATLAB/Simulink were compared.

## *Conclusion*

## *General Conclusion*

In this thesis, we studied a wind energy conversion chain based on a permanent magnet synchronous generator. This system consists of a turbine coupled to a permanent magnet synchronous generator, along with a PWM static converter on the generator side.

In order to improve the performance and control of the operation of the permanent magnet synchronous generator, the work presented in this thesis aims to achieve the following objectives:

The first part focuses on the use of the permanent magnet synchronous machine controlled by its stator-side converter (SSC). The modeling involves a two-level converter on the stator side (SSC) for harnessing wind energy.

The second objective focused on improving the quality of the voltage supplied to the rectifier by the PMSG. To enhance this voltage, a predictive control technique was applied to optimize the voltage value with the aim of minimizing the error between the reference value and the measured value. The simulation results demonstrated a significant improvement in voltage performance.

In the third chapter, the hybrid control strategy that combines Field-Oriented Control (FOC) with Model Predictive Control (MPC) offers a powerful and efficient solution for optimizing the performance of Permanent Magnet Synchronous Motors (PMSMs) in wind turbine applications.

Based on these observations and the results obtained, and in order to provide a definitive assessment of these control techniques, several research perspectives are proposed that could contribute to the enhanced exploitation of wind energy conversion systems:

- ✓ The simulation results should be validated by experimental tests on a test bench.
- ✓ In order to develop and improve the dynamic performance of drive and control systems, it is suggested to study and implement the **Root Tree Optimization (RTO)** technique to optimize the voltage value of the PWM rectifier.

# References



- [Abd 18] Abdelhamid BOUHELAL ;"*Contribution to the aerodynamic study of the air-sand flow around a wind turbine blade* (Doctoral dissertation) "; Ecole Nationale Polytechnique, Algier;2018.
- [Ade 07] Adel Merabet, "Commande Non Linéaire à Modèle Prédictif pour une Machine Synchrone", Québec, Mai 2007.
- [Aid 13] Aid. H, W.Aina;"Synthèse De Lois De Commande Non-Linéaires Pour Un Entraînement Electrique A Vitesse Variable Basé Sur Un Moteur Synchrone A Aimants Permanents "; Mémoire De Master, Université Abou Bekr Belkaid, Tlemcen, 2013.
- [Ala 02] Alaoui. M ;"Commande Et Observateur Par Mode Glissant D'un Système De Pompage Et D'un Bras Manipulateur "; Thèse De Doctorat, Université De Sidi Mohammed Ben Abdallah;2002.
- [Alb 04] Albán. O.A.V;"Contribution à l'identification et à la commande des robots parallèles"; thèse de doctorat, Université MONTPELLIER II; 2004.
- [All 17] Allag Abd Elkarim ;"Commande par mode glissant flou d'une machine synchrone à aimants permanents"; L'Université Echahid Hamma Lakhdar d'El Oued; 2017.
- [Ami 17] Amiri. M Ali Dahmane. O ;"Commande Vectorielle En Vitesse Du Moteur Synchrone A Aimants Permanents Dotée D'un Observateur Mode Glissant " ;Thèse De Master, Université AboubakrBelkaïd– Tlemcen –;Soutenu 04 / 07 / 2017.
- [Ami 07] Amirouche. N.S ;"Contribution A La Commande Adaptative Et Neuronale D'une Machine Synchrone A Aimants Permanents " ;Thèse De Doctorat, Ecole Nationale Polytechnique; 2007.
- [Att 11] Attou. M Amine ;" Commande Par Mode De Glissement de la MSAP";Thèse de Mastère , Université Djilali Liabes De Sidi Bel Abbes ; 2011.
- [Aya 17] AYADI Mohammed ;"Commande d'une machine synchrone à aimants permanents par logique floue";Université Echahid Hamma Lakhdar d'El-Oued;2017.

## B

- [Bel 01] Belabbes. B ;"Commande Linéarisant D'un Moteur Synchrone A Aimants Permanents " ; Mémoire De Magister, Université Djilali Liabes De Sidi Bel Abbes, Algérie ; 2001.
- [Bel 14] Belkhir. K. S;"Application of magnetic power-split device / CVT to variable speed wind turbine for wind power generation (Doctoral dissertation) ";University Ferhat Abbas - Setif 1;2014.
- [Ben 05] Benchabane. F;" Commande en position et en vitesse par mode de glissement d'un moteur synchrone triphasé à aimants permanents avec minimisation du chattering"; Thèse de magistère, Université de Biskra; 2005.
- [Ben 22] BENNOUNA . M. S; " Commande de la vitesse d'une machine synchrone à aimant permanent à double étoile par logique floue";university kasdi merbah ouargla;2022.
- [Bou 06] Bouchafaa. F;" Etude et Commande de différentes Cascades à Onduleur à Neuf Niveaux à Structure NPC. Application à la conduite d'une MSAP"; Thèse de doctorat,Ecole nationale polytechnique, El-Harrach; 2006.
- [Bou 14] BOUDJEMA, A. R. (2014). Commande vectorielle de la machine synchrone à aimants permanents MSAP (Master's thesis).
- [Bou 12] BOUKAIS. B "Contribution à la modélisation des systèmes couples machines convertisseurs: Application aux machines à aimant permanents (BDCM – PMSM),Thèse de l'université de Mouloud Mammeri, Tizi-Ouzou, 21 Fév.2012.
- [Bou 22] BOUMAZA Yazid KOBSI Karim;" Minimisation de la dégradation des Moteurs PMSM par Contrôleurs PI et MPC ";NIVERSITÉ BADJI MOKHTAR – ANNABA;2022.
- [Bri 13] Brill. B. I. (2002, November 19). "Modular wind energy device"; Free Patents Onlin; Retrieved November 6, 2013.

## C

- [Cam 03] Camacho. E.F, C.Bordons, "Model Predictive Control", Springer-Verlag London, 2eme edition, 2003.
- [Cha 06] Chakir. M ;" Commande Robuste Tolérante aux Défauts Application à la MSAP"; Thèsede magistère, Ecole nationale polytechnique, El-Harrach ;2006.

- [Cla 87] Clarke. D.W, C. Mohtadi et p.s, Tuffs, 1987; Generalized predictive control; part I and, Automatica; vol, 23, N2, pp-137-160.

## D

- [Del 21] Debal. A ;"Commande Vectorielle De La MSAP En Utilisant La Technique Mli Vectorielle ";Mémoire De Master De Université Labri Ben M'Hidi-Oum El-Bouaghi Soutenu Le 14/07/2021.
- [Djo 15] Djouder. M ;"Modélisation Et Commande D'un Véhicule Electrique A Base D'une Machine Synchrone A Aimants Permanents "; Mouloud Mammeri Université Tizi-Ouzou Algérie Thesis ;Septembre 2015.

## E

- [Ens 02] Enso Ikonen, Kaddour Najim, " Advanced Process Identification and Control", Marcel Dekker, New York.Bsel, 1ere edition, 2002.

## G

- [Gan 21] Ganthia. B. P., Barik, S. K., & Nayak, B. "Wind turbines in energy conversion system: Types & techniques"; In Renewable energy and future power systems (pp. 199-217). Singapore: Springer Singapore;2021.
- [Garr 01] Garrad Hassan & Partners, Bristol, UK; " *Wind Energy Handbook*"; UMIST, Manchester,UK;2001.
- [Guy 00] Guy. G, et Guy. G; "Actionneurs Electriques, Principes Modèles Commande"; Edition Eyrolles; 2000.

## J

- [Jha 11] Jha. A. R. ; "Wind turbine technology";CRC press;2011.

## K

- [kad 00] Kaddouri. A;" Étude d'une commande non-linéaire adaptative d'une machine synchrone à aimants permanents"; Thèse de doctorat Philosophie, Université

LAVAL QUÉBEC Canada; 2000.

- [Ker 21] KERROUCHE Mohammed ;"Commande prédictive d'une Génératrice Synchrone à aiment permanent"; Université Echahid Hamma Lakhdar d'El-Oued ;2021

## M

- [Mah 12] Mahgoun. M.S ;"Application De La Commande  $H_{\infty}$  Aux Systèmes Linéaires Perturbés "; Mémoire De Magister, Université Ferhat Abbas-Setif ; 2012.
- [Mal 00] Malhoud. Maaziz, "Commande prédictive de systèmes non linéaires application à la commande de machines asynchrones", Thèse de Doctorat université Paris Xi Orsay, 2000.
- [Mal 10] Mallet. J, « PID versus PFC », article, 2010.
- [Mar 16] MARIA SANDSTRÖM ; " Master's thesis in the Sustainable Energy Systems programme"; Hólmfríður Haraldsdóttir (Supervisor), Department of Energy and Environment, Division of Electric Power Engineering, Chalmers University of Technology. Göteborg, Sweden;2016.
- [Mel 22] MELIK Mohammed ;"WIND TURBINES-COMPONENT AND DESIGN BASICS "; EchahidHamma University of El-OuedLakhdar; 2022.
- [Mer 07] Merzoug. M.S ;"Etude Comparative Des Performances D'un DTC Et D'un FOC D'une Machine Synchrone A Aimants Permanents (MSAP) "; Mémoire De Magister, Batna, Algérie; 2007.
- [Mig 04 ] MIGLIORE.E. G, " Commande Prédictive à Base de Programmation Semi Définie", thèse de doctorat, l'Institut National des Sciences Appliquées de Toulouse, 2004.

## N

- [Nai 07] Nait Seghir. A;" Contribution a la commande adaptative et neuronale d'une machine synchrone à aimants permanents "; Thèse de doctorat, Ecole nationale polytechnique, ElHarrach;2007.
- [Nic 06] Nicolas Petit,Commande prédictive, Notes de cours, école centrale Paris, Année Scolaire 2005-2006.

## P

- [Pat 96] Patrick Boucher, Didier Dumur, "la commande prédictive", collection méthodes et pratiques de l'ingénieur, école centrale de Lille, 1996.

## S

- [Sad 20] Sadrehaghighi, I; "Wind Turbines";2020
- [Sek 08] Sekkel. A.S "Etude Comparative Des Diéreses Commandes De La Machine A Aimants Permanents " Mémoire de Magister, Université Djilali Liabes SBA, Algérie, 2008.
- [Ser 09] Serhoud. H; "Contribution A L'étude De La Machine Synchrone A Réductance Variable "; Thèse Magister De Université De Batna Soutenu Le,01/07/2009.
- [Sha 16] Shaikh. H. A; "Renewable energy"; Retrieved from; <https://www.academia.edu/search?q=energy%20renewable%20doc> ;2016.
- [Sid 97] Siddig. M. H ;"The feasibility of using wind-pumps in Zimbabwe"; *Wind Engineering*, 227-236;1997.
- [Szl 17] Szlivka. F. Molnár, I., & Sándor, G;"ADVANTAGES AND DISADVANTAGES OF DIFFERENT TYPES OF WIND TURBINES AND THEIR USAGE IN THE CITY";*on Wind Energy Harvesting*;2017.

## T

- [Tho 05] Thomas Ackermann; " Wind Power in Power Systemes" ;Royal Institute of Technology Stockholm, Sweden;2005.

## Y

- [Yah 05] Yahia. K;" Estimation en ligne de l'état et des paramètres du moteur asynchrone triphasé";Thèse de magistère, Université de Biskra;2005.

# Annexe

## A. Paramètres de la Génératrice

Tableau. A. Paramètres de la Génératrice

<i>Nom et symbole des paramètres</i>	<i>Valeur numérique</i>
<i>La puissance nominal <math>P</math></i>	<i>1.5 KW</i>
<i>La tension nominal <math>V</math></i>	<i>220 V</i>
<i>La résistance de la phase statorique <math>R_s</math></i>	<i>0.6 <math>\Omega</math></i>
<i>Inductance directe <math>L_d</math></i>	<i>0.0014 H</i>
<i>L'inductance quadrature <math>L_q</math></i>	<i>0.0028 H</i>
<i>Moment d'inertie total de la machine <math>J</math></i>	<i>0.02Kg m<sup>2</sup></i>
<i>Coefficient de frottement visqueux <math>f</math></i>	<i>0.0014 N.m/rd/s</i>
<i>Le nombre de paires de pôles <math>P</math></i>	<i>4</i>
<i>La résistance de charge <math>R_{ch}</math></i>	<i>10 <math>\Omega</math></i>
<i>L'inductance de charge <math>L_{ch}</math></i>	<i>0.002 H</i>
<i>Flux d'excitation des aimants <math>\Psi_f</math></i>	<i>0.8 Wb</i>

## B. Paramètres de Turbine

Tableau. B. Paramètres de la turbine éolienne

<i>Nom et symbole des paramètres</i>	<i>Valeur numérique</i>
<i>Gain du multiplicateur de vitesse <math>G</math></i>	<i>6</i>
<i>Rayon de la turbine <math>R</math></i>	<i>3</i>
<i>Masse volumique de l'air <math>\rho</math></i>	<i><math>\rho = 1.22(Kg/m^3)</math></i>
<i>Rayon de la turbine <math>R_t</math></i>	<i>3m</i>
<i>Inertie de l'arbre <math>J</math></i>	<i>0.21Kg. m<sup>3</sup></i>

## C. Paramètres de redresseur

*Tableau. C. Paramètres de redresseur*

<b>Nome et symbole des paramètres</b>	<b>Valeur</b>
<i>La résistance</i>	$R=6\Omega$
<i>La capacité</i>	$C=0.0033Var$
<i>l'inductance</i>	$L=0.0014 H$

